JAERI-Research
95-037

CREEP BEHAVIOUR OF HASTELLOY XR IN SIMULATED HIGH-TEMPERATURE GAS-COOLED REACTOR HELIUM

June 1995

Yuji KURATA, Yutaka OGAWA*, Tomio SUZUKI
Masami SHINDO, Hajime NAKAJIMA and Tatsuo KONDO**

日本原子力研究所
Japan Atomic Energy Research Institute

本レポートは，日本原子力研究所が不定期に公刊している研究報告書です。
入手の問合わせは，日本原子力研究所技術情報部情報資料課（〒319-11 茨城県那珂郡東海村）あて，お申し越しください。なお，このほかに財団法人原子力弘済会資料センター（〒319-11 茨城県那珂郡東海村日本原子力研究所内）で複写による実費頒布をおこなっております。

This report is issued irregularly.
Inquiries about availability of the reports should be addressed to Information Division, Department of Technical Information, Japan Atomic Energy Research Institute, Tokai-mura, Naka-gun, Ibaraki-ken 319-11, Japan.

編集兼発行　日本原子力研究所
印　　刷　㈱原子力資料サービス

Creep Behaviour of Hastelloy XR in Simulated High-temperature Gas-cooled Reactor Helium

Yuji KURATA, Yutaka OGAWA* ,Tomio SUZUKI
Masami SHINDO, Hajime NAKAJIMA+ and Tatsuo KONDO**

Department of Materials Science and Engineering
Tokai Research Establishment
Japan Atomic Energy Research Institute
Tokai-mura, Naka-gun, Ibaraki-ken

(Received April 25, 1995)

Creep tests of Hastelloy XR (a modified version of the conventional Hastelloy X) were carried out in simulated high-temperature gas-cooled reactor helium at 800, 900 and 1000℃. The test results up to about 50,000h showed no significant degradation in creep properties such as the rupture life, rupture ductility and the steady-state creep rate. The creep-rupture strength obtained through long-term tests was above the level corresponding to the design allowable creep-rupture stress of the High-Temperature Engineering Test Reactor. The values of the stress exponent were 4.5 to 5.7 when the stress dependence of the steady-state creep rate was expressed in terms of the Norton equation. Rupture lives could be estimated with sufficient accuracy using Larson-Miller parameter. Carbon analysis for ruptured specimens showed that carburization was limited to the region near the ruptured portion. The surface crack tips were blunted at the depth of 100 to 200 μm from the specimen surface. Internally formed cracks were initiated at sites of precipitates at grain boundaries, growing nearly perpendicular to the stress axis. The electron probe microanalysis revealed that two precipitates, Mo-rich phase and Cr-rich phase, co-existed.

+ Office of Planning
* Research Institute for Metals, Tohoku University
** Tohoku University

Keywords: Creep, HTGR Helium, HTTR, Rupture Life, Rupture Ductility, Steady-state Creep Rate,Design Allowable Stress,Norton Equation,Larson-Miller Parameter, Carburization, Crack, Grain Boundary,Precipitate

高温ガス炉近似ヘリウム中におけるハステロイＸＲのクリープ挙動

日本原子力研究所東海研究所材料研究部
倉田　有司・小川　豊*・鈴木　富男
新藤　雅美・中島　甫+・近藤　達男**

（1995年４月25日受理）

800，900及び1000℃の高温ガス炉近似ヘリウム中でハステロイＸＲのクリープ試験を行った。約50,000時間までの試験結果は，破断寿命，破断延性，定常クリープ速度のようなクリープ特性の著しい劣化を示さなかった。長時間試験により得られたクリープ破断強度は高温工学試験研究炉の設計クリープ破断応力強さに対応する強度水準を十分上回っていた。定常クリープ速度の応力依存性をNorton式で表したとき，応力指数の値は4.5～5.7であった。破断寿命はLarson－Millerパラメータにより十分な精度で評価することができた。破断した試料の炭素分析は浸炭が破断部近傍に制限されることを示した。表面クラックの先端は鈍化しており，その深さは 100～200 μmであった。内部に形成したクラックは応力軸に垂直な粒界で成長した析出物付近で発生していた。電子線マイクロアナライザーによる分析により，長時間クリープ破断材で，Ｍｏに富んだ析出物とＣｒに富んだ析出物が共存していることがわかった。

東海研究所：〒319-11　茨城県那珂郡東海村白方白根２－４
+ 企画室
* 東北大学金属材料研究所
**東北大学

Contents

目　　次

1. Introduction

High-temperature gas-cooled reactors, which use helium gas as the primary coolant, are believed to be one of the most promising systems with inherent safety and high thermal efficiency. A reactor named High-Temperature Engineering Test Reactor (HTTR) is currently under construction as the first attempt in Japan[1,2]. Creep properties are among the important basic items of material performance to be considered in high-temperature structural design of the HTTR. In nuclear reactor applications, the projected life of the primary circuit is generally long, e. g. 10^5 h. A highly accurate and dependable data base is, therefore, required to allow reasonable life prediction and safety assessment during the service life.

Pure helium gas is inert. However, the primary coolant helium, which passes through the large mass of hot graphite core structure, cannot avoid containing slight amount of impurity gases, i. e., H_2, H_2O, CO, CO_2 and CH_4. It is considered that these impurities can cause oxidation and carburization or decarburization in heat-resistant alloys and possible effects upon creep properties are suspected. For this reason many research works on creep tests in flowing helium containing a small amount of impurities have been carried out[3 -12]. While investigators showed that creep rupture lives of certain alloys become shorter in impure helium than in air[3,4,7], it was also reported that in some cases there is little significant difference between impure helium and air in creep rupture lives[5-12]. These different results were considered to be caused by either singular or combined effects of differences in chemical composition of alloys used for experiments, in impurity composition in the helium environment and in the gas flow rate. Therefore, authors have conducted creep tests in simulated HTGR helium with special care on impurity

chemistry in helium.

An intermediate heat exchanger(IHX) of the HTTR is being manufactured using Hastelloy XR (a modified version of the conventional Hastelloy X). High temperature components such as the IHX were designed using High-Temperature Structural Design Code[13] and Design Allowable Limits[14]. At the time of the design of the HTTR a lot of creep data were used to generate the Design Allowable Limits for which the allowable stress for long-time service was determined through some reasonable extent of extrapolation from the test data obtained up to that time. The confirmation of whether the allowable stress is sufficiently marginal or not is meaningful when creep data in longer tests are obtained.

The authors reported that there was no significant difference between helium and air in the creep rupture lives obtained at 800 to 1000℃ up to about 10,000h and that the test results showed no significant degradation in creep properties[11,12]. In this paper, the behaviour for further extended time including creep data up to about 50,000h is described in conjunction with carburization behaviour and results of microstructural observation.

2. Experimental procedure

2.1Specimens

The material tested in this study is Hastelloy XR developed for high temperature components of the HTTR. Hastelloy XR is an improved version of Hastelloy X, which has been used for Oarai Gas Loop 1 of Japan Materials Testing Reactor. Table 1 shows chemical composition of Hastelloy XR together with the specification of Hastelloy X(ASTM B435). Hastelloy XR has a basal composition for the major constituents common with that of Hastelloy X (i.e., nominally Ni-22Cr-18Fe-9Mo in mass %), while contents of specific minor elements are optimized: Mn and Si are adjusted in the optimum ranges and

chemistry in helium.

An intermediate heat exchanger(IHX) of the HTTR is being manufactured using Hastelloy XR (a modified version of the conventional Hastelloy X). High temperature components such as the IHX were designed using High-Temperature Structural Design Code[13] and Design Allowable Limits[14]. At the time of the design of the HTTR a lot of creep data were used to generate the Design Allowable Limits for which the allowable stress for long-time service was determined through some reasonable extent of extrapolation from the test data obtained up to that time. The confirmation of whether the allowable stress is sufficiently marginal or not is meaningful when creep data in longer tests are obtained.

The authors reported that there was no significant difference between helium and air in the creep rupture lives obtained at 800 to 1000℃ up to about 10,000h and that the test results showed no significant degradation in creep properties[11,12]. In this paper, the behaviour for further extended time including creep data up to about 50,000h is described in conjunction with carburization behaviour and results of microstructural observation.

2. Experimental procedure

2.1Specimens

The material tested in this study is Hastelloy XR developed for high temperature components of the HTTR. Hastelloy XR is an improved version of Hastelloy X, which has been used for Oarai Gas Loop 1 of Japan Materials Testing Reactor. Table 1 shows chemical composition of Hastelloy XR together with the specification of Hastelloy X(ASTM B435). Hastelloy XR has a basal composition for the major constituents common with that of Hastelloy X (i.e., nominally Ni-22Cr-18Fe-9Mo in mass %), while contents of specific minor elements are optimized: Mn and Si are adjusted in the optimum ranges and

Al, Ti and Co are reduced to the possible lowest levels[15]. The material was supplied in the form of bars of 15 mm in diameter. The solution treatment temperature of the bars was 1180℃ and the grain size was ASTM No.3-4. Specimens of 6 mm in diameter and 30 mm in gauge length were used for creep tests. Geometry of the specimen for the creep test in helium environment is shown in Fig. 1.

2.2 Test environment and apparatus

Creep tests were carried out in helium environment designated as JAERI Type B helium, which was one of the experimental specifications of the simulated HTGR primary coolant environments. Impurity composition of JAERI Type B helium is shown in Table 2. Here, the ratio of H_2 to H_2O is 170 to 260 and the ratio of CO to CO_2 is 30 to 55. The chemical characteristic of this impure helium environment is low oxidizing and slight carburizing for Hastelloy XR. The helium gas was supplied to each creep machine by the helium circulation loop with functions of purification and impurity addition . The helium gas was introduced with a supply rate at or above 150 ml/min per 1 cm^2 of the specimen surface area (total 1 l/min). A hygrometer was used for measurement of H_2O in the helium environment, and a gaschromatograph for that of other impurities.

Single specimen type uniaxial creep machines[16], specially designed for a helium environment as described below, were used. Special care was exercised in avoiding undesirable perturbation of the local impurity composition at the test section due either to degassing from or to reaction with the machine components. Figure 2 shows the cross section of the creep machine. Features of the machine are as follows;

1. Structural components exposed to high-temperature helium are made of quartz, molybdenum and nickel, all chemically inert in the given helium

environment.

2. A contamination-free optical creep strain measuring device (i.e., a grated quartz interferometer attached to the gauge section) was developed for the machine.

Creep tests in the helium environment were carried out at 800, 900 and 1000℃, and under 6.9 to 98.1 MPa. During the test, the temperature was monitored by platinum/platinum-rhodium thermocouples attached along the specimen gauge section.

3. Results and discussion

3.1 Creep properties

Figure 3 shows the relationship between stress and time to rupture for Hastelloy XR in JAERI Type B helium. The solid lines are the expected mean values of the Design Allowable Limits[14], and the broken lines the design allowable creep-rupture stress (S_R) of the Design Allowable Limits[14]. It can be said that the strength level of the creep-rupture data including results of creep tests up to 48,557.5h is equal to that of the expected mean values. It is above S_R at each temperature and long-term data above 10,000 h show no significant degradation in creep rupture lives. The relationship between rupture elongation and time to rupture at 800, 900 and 1000℃ is shown in Fig. 4. Reduction of area vs. time to rupture is also shown in Fig. 5. While rupture ductility generally decreases with increasing rupture time, the results shown in Figs. 4 and 5 have a tendency of leveling off in the decrease of rupture ductility after a few thousand hours.

Examples of strain(nominal strain) vs. time plots tested at 800℃ are shown in Fig. 6(a) to 6(d). Similar results tested at 900 and 1000℃ are also indicated in Fig. 7(a) to 7(f) and in Fig. 8(a) to 8(d), respectively. Creep curves in long-term tests at 800, 900 and 1000℃ are shown in Fig. 9. It was reported

environment.

2. A contamination-free optical creep strain measuring device (i.e., a grated quartz interferometer attached to the gauge section) was developed for the machine.

Creep tests in the helium environment were carried out at 800, 900 and 1000℃, and under 6.9 to 98.1 MPa. During the test, the temperature was monitored by platinum/platinum-rhodium thermocouples attached along the specimen gauge section.

3. Results and discussion

3.1 Creep properties

Figure 3 shows the relationship between stress and time to rupture for Hastelloy XR in JAERI Type B helium. The solid lines are the expected mean values of the Design Allowable Limits[14], and the broken lines the design allowable creep-rupture stress (S_R) of the Design Allowable Limits[14]. It can be said that the strength level of the creep-rupture data including results of creep tests up to 48,557.5h is equal to that of the expected mean values. It is above S_R at each temperature and long-term data above 10,000 h show no significant degradation in creep rupture lives. The relationship between rupture elongation and time to rupture at 800, 900 and 1000℃ is shown in Fig. 4. Reduction of area vs. time to rupture is also shown in Fig. 5. While rupture ductility generally decreases with increasing rupture time, the results shown in Figs. 4 and 5 have a tendency of leveling off in the decrease of rupture ductility after a few thousand hours.

Examples of strain(nominal strain) vs. time plots tested at 800℃ are shown in Fig. 6(a) to 6(d). Similar results tested at 900 and 1000℃ are also indicated in Fig. 7(a) to 7(f) and in Fig. 8(a) to 8(d), respectively. Creep curves in long-term tests at 800, 900 and 1000℃ are shown in Fig. 9. It was reported

that normal type creep curves consisting of transient, steady-state and accelerated stages were observed at 800℃ and that, for Hastelloy XR at 1000 ℃, some irregular creep curves were often observed [17,18]. In the present case, while long-term creep curves at 800 and 900℃ are normal type curves as shown in Fig. 9, the creep curve at 1000℃ is the irregular creep curve where the transient stage is hardly recognized. Figure 10 shows the relationship between the steady-state creep rate and stress. The creep rate at 3% strain was adopted as the steady-state creep rate when the steady-state region was not recognized clearly in the irregular creep curves.

The relationship between the steady-state creep rate, $\dot{\varepsilon}_s$, and stress, σ, is generally expressed as a power law, often called Norton's Law [19].

$$\dot{\varepsilon}_s = A\,\sigma^n \qquad (1)$$

where n is the stress exponent and A constant. Taking logarithms leads to :

$$\log \dot{\varepsilon}_s = A' + n \log \sigma \qquad (2)$$

The following equations are obtained applying the least squares method to data at each temperature.

800℃: $\log \dot{\varepsilon}_s = -12.3166 + 5.747242 \log \sigma$ (2-a)

900℃: $\log \dot{\varepsilon}_s = -8.9716 + 4.685546 \log \sigma$ (2-b)

1000℃ : $\log \dot{\varepsilon}_s = -7.0646 + 4.527191 \log \sigma$ (2-c)

The stress exponent, n, at each temperature does not change within this experimental condition even if the stress decreases. It was reported that n would be unity under the diffusional creep mechanism and that n would be greater than 3 under the dislocation creep mechanism[20]. The creep process of Hastelloy XR within this experimental condition is interpreted to be dominated by the dislocation creep mechanism since n values are above 3.

The n value is about 5.7 at 800℃ and it decreases to about 4.5 at 1000℃. Generally the n value is about 5 for solution-strengthened alloys, and it is often above 5 for precipitation-strengthened alloys[21]. Hastelloy XR is strengthened mainly by solution and additionally by precipitation. The facts that the n value is above 5 at 800℃ and that it decreases with increasing temperature are explained by the decrease in the function of precipitation strengthening due to the coarsening of precipitates at high temperatures.

The Norton equation can be modified to enable the temperature dependence of the steady-state creep rate to be represented in terms of a parameter, Qc, activation energy for creep.

$$\dot{\varepsilon}_s = K \sigma^n \exp(-Qc/RT) \qquad (3)$$

where R is the gas constant, T absolute temperature and K constant. An estimated magnitude of Qc can be derived from a plot of log $\dot{\varepsilon}_s$ against (1/T) at constant stress as shown in Fig. 11. The Qc values obtained for data under 19.6, 39.2 and 51.0 MPa were 340-450 KJ/mol. These values are larger than the value, 280 KJ/mol[22], of lattice self-diffusion in pure-Ni. By these approaches, we can say that dislocation creep with n values of about 5 and with Qc values larger than activation energy for lattice self-diffusion in pure Ni is predominant under conditions applied in this study.

Not only time to rupture but also time to 1% total strain and time to onset of tertiary creep were used to generate the allowable stress(St) of Design Allowable Limits[14]. Figure 12 shows stress vs. time to 1% total strain and time to rupture for Hastelloy XR tested in JAERI Type B helium. Since measurement of initial strain in helium environment is difficult, time to 1% total strain is not necessarily measured with enough accuracy. Stress vs. time to onset of tertiary creep is also shown in Fig.13. These creep properties are indicated in Table 3 to 5.

3.2 Prediction of long-term creep rupture lives

The following Monkman-Grant equation[23] is useful to perform the prediction of life or residual-life of high-temperature component.

$$\log t_R = c - m \log \dot{\varepsilon}_s \quad (4)$$

where t_R is time to rupture, c and m are constants. Figure 14 shows the relationship between the time to rupture and the steady-state creep rate for Hastelloy XR. The following equations were obtained by applying the least squares method to data obtained at each temperature or at all temperatures.

800℃: $\log t_R = 1.121561 - 0.98461 \log \dot{\varepsilon}_s$ (4-a)

900℃: $\log t_R = 1.351468 - 0.95116 \log \dot{\varepsilon}_s$ (4-b)

1000℃: $\log t_R = 1.697157 - 0.75331 \log \dot{\varepsilon}_s$ (4-c)

All : $\log t_R = 1.398525 - 0.90125 \log \dot{\varepsilon}_s$ (4-d)

These regression curves are also shown in Fig. 14. Generally, longer rupture lives are predicted in the Monkman-Grant relationship when rupture elongation is large. Because rupture ductility of Hastelloy XR does not decrease in long-term test in JAERI Type B helium at 800 and 900℃ (see Figs. 4 and 5), the m values of equation(4) are large and then longer rupture lives are predicted under lower stresses. The m values decrease with increasing temperature. The regression curve for data at all temperatures approaches to that for data at 900℃. Creep rupture lives for Hastelloy XR can be predicted using the Monkman-Grant equation.

The time-temperature parameter (TTP) method is often used to analyze creep-rupture data and to predict rupture life and stress[24,25]. In present study, the following parameters were investigated.

Larson-Miller: $LMP = T(C + \log t_R)$ (5)

Orr-Sherby-Dorn: $OSDP=\log t_R - Q/19.1425T$ (6)

where C and Q are parameter constants. Equation $f(\sigma)$, which represents stress dependence of TTP, is approximated using polynomials of logarithmic of stress as

$$f(\sigma)=b_0+b_1\log(\sigma)+b_2(\log(\sigma))^2+\cdots+b_k(\log(\sigma))^k \quad (7)$$

where b_0, b_1,b_2, $\cdots$, b_k are regression constants. Parameter constants in equations (5)-(7) are optimized to minimize standard error of estimate (SEE) of $\log t_R$.

$$SEE=\sqrt{\Sigma(Yi - \hat{Y}i)^2/(n_d - n_p-k-1)} \quad (8)$$

where Yi is a measured value of $\log t_R$, $\hat{Y}i$ an estimated value of $\log t_R$, n_d the number of data points, n_p the number of parameter constant in TTP and k the degree of equation (7). The optimization procedure was carried out following the study on standardization of creep-rupture data evaluation of metals [25]. Table 6 shows results of TTP analysis for Hastelloy XR. It is found that the degree of polynomials is 2 for LMP and OSDP to have good approximation. Furthermore, the application of LMP results in better fit than that of OSDP. On this basis the results obtained from analysis in terms of LMP are shown in Fig. 15. Solid lines are regression curves obtained from application of LMP to all data. These curves fit experimental results containing long-term data.

Since design lives of components are very long (10^5 h), extrapolation from experimental data is employed to generate the design allowable stress. For this reason, it is necessary to confirm whether the design allowable stress is sufficiently marginal for safety with long-term data when they are obtained. In addition, it is important to investigate to what extent extrapolation is possible. The former has been confirmed in Section 3.1. The latter is

examined here. The broken lines in Fig. 15 are regression curves obtained from application of LMP to the data below 5,000 h. The degree of extrapolation is estimated using root mean squares (RMS) as

$$RMS=\sqrt{\Sigma(Yj - \hat{Y}j)^2/(n_e - 1)} \qquad (9)$$

where n_e is the number of long-term data which were not used for calculation of TTP analysis. Yj is actual data of long-term tests and $\hat{Y}j$ is the value estimated by TTP using data below 5,000 h. It can be said that reliable extrapolation is performed if RMS values are small and the difference between RMS and SEE values is small. As shown in Table 7, RMS value is considerably larger than SEE value in the case of extrapolation using the data below 5,000 h and thus the reliability of this extrapolation is not sufficient. As shown in Fig. 15, the regression curves obtained from the extrapolation using the data below 5,000 h predict shorter rupture lives at 1000℃ and low stresses than those obtained by experiments. It is found that longer creep rupture data should be used for TTP analysis to enable accurate prediction of long-term creep rupture lives.

3.3 Carbon analysis and microstructure observation

Since carburization and decarburization have appreciable effects on creep behaviour [4,7,26,27], carbon analysis was carried out for ruptured specimens. Furthermore, microstructure observation for surface and cross sections of ruptured specimens was performed.

Figure 16 and Table 8 show results of carbon analysis. Carbon content was analyzed for section including rupture portion where there are many cracks and for 8-mm-diameter section where there is little creep deformation. Carbon content in the former is high as shown in Fig. 16 and Table 8. This tendency becomes significant with higher temperatures and longer times. On the other hand, there is only a little carburization in 8-mm-diameter section

even after long-term exposure to the impure helium. It can be said that carbon intrusion during the steady-state creep stage was limited to a negligible level even if significant carburization occurred in the section around rupture portion.

Photos. 1 and 2 show surface topography of Hastelloy XR creep-ruptured in JAERI Type B helium. It is recognized that there are many surface cracks which grow in the direction perpendicular to the stress direction at 800 and 900℃. On the other hand, large surface cracks were observed at 1000℃ as shown in Photos. 1(f) and 2(c). Surface corrosion products formed at 1000 ℃ are of blocky type and different from those formed at 800 and 900℃[12]. Photo. 3 shows microstructures of Hastelloy XR creep-ruptured in JAERI Type B helium. Small surface cracks along grain boundaries are observed at 800℃ in Photo. 3 (a). Surface cracks become large with increasing temperature. The depth of the surface crack was about 100-150 μm at 800 and 900℃, and about 200 μm at 1000℃. Since the crack tips were blunted at the depth of 100 to 200 μm from the specimen surface, it is judged that the surface cracks were not the predominant cause of failure[28]. Extensive recrystallization was observed at 1000℃ while small recrystallized grains were locally observed at 900℃. Internally formed cracks were initiated at the sites of carbide precipitation at grain boundaries. Grain boundaries perpendicular to the stress axis are under tensile stress. Precipitates at grain boundaries under tensile stress coarsen at 1000℃ and there are little precipitates in matrix or at grain boundaries parallel to the stress axis while there are many precipitates in matrix and grain boundaries at 800℃. It was reported for Inconel 617 that precipitates at grain boundaries under tensile stress coarsen [29]. The coarsened precipitates, which localized at grain boundaries under tensile stress, would have little effect on creep strength. Photos 4, 5 and 6 show scanning electron micrographs of Hastelloy XR ruptured at 800, 900 and 1000 ℃, respectively. The electron probe microanalysis revealed that two phases

co-existed at 1000℃: ①Mo-rich phase presumed to be M_6C type carbide[30] and ②Cr-rich phase presumed to be $M_{23}C_6$ type carbide[30]. Table 9 shows the results of quantitative analysis of precipitates and matrix of Hastelloy XR ruptured in 13,014 h at 1000℃. While bright precipitates shown in Photo. 6 are Mo-rich phase, dark precipitates are Cr-rich phase. The two phases were also found at 800 and 900℃. However, the contents of Mo and Cr were somewhat different from those at 1000℃. A lot of bright precipitates were observed at 800 and 900℃ as shown in Photos. 4 and 5.

4. Conclusions

Creep tests of Hastelloy XR were carried out in simulated HTGR helium up to about 50,000 h at 800, 900 and 1000℃. The main results obtained are as follows:

(1)The test results up to about 50,000 h showed no significant degradation in creep properties such as the rupture life, rupture ductility and the steady-state creep rate. Creep-rupture stress is substantially above S_R of the Design Allowable Limits.

(2)The stress dependence of the steady-state creep rate is expressed in terms of the Norton equation. The values of the stress exponent is 4.5 to 5.7. On this basis, it is judged that dominant creep process is dislocation creep.

(3)The relationship between the steady-state creep rate and time to rupture is expressed in terms of the Monkman-Grant equation. The equation is found to be successfully used for life prediction of high temperature components manufactured using Hastelloy XR.

(4)Rupture lives of Hastelloy XR can be estimated with sufficient accuracy using a Larson-Miller parameter. Since TTP analysis using data below 5,000 h predicts low rupture lives at high temperature and low stress, it is necessary to use longer creep-rupture data for TTP analysis in order to enable accurate prediction of long-term creep rupture lives.

(5)Although some appreciable carburization was recognized in the specimens ruptured after creep tests in JAERI Type B helium, the slight carbon intrusion detected was seen to have occurred only in the early stage of exposure during the steady-state creep stage . On the other hand, significant carburization occurred in the section including rupture portion.

(6)The surface crack tips were blunted at the depth of 100 to 200 μm from the specimen surface. Internally formed cracks were initiated at sites of precipitates at grain boundaries, growing nearly perpendicular to the stress axis.

(7)The electron probe microanalysis revealed that two phases co-existed :① Mo-rich phase presumed to be M_6C type carbide and ②Cr-rich phase presumed to be $M_{23}C_6$ type carbide.

Acknowledgements

Authors are very grateful to staffs of Material Performance and Testing Laboratory for their assistance during this long-term study.

(7)The electron probe microanalysis revealed that two phases co-existed :① Mo-rich phase presumed to be M_6C type carbide and ②Cr-rich phase presumed to be $M_{23}C_6$ type carbide.

Acknowledgements

Authors are very grateful to staffs of Material Performance and Testing Laboratory for their assistance during this long-term study.

References

(1)Japan Atomic Energy Research Institute : Present Status of HTGR Research and Development (1992).

(2)Japan Atomic Energy Research Institute : Present Status of HTGR Research and Development (1994) [in Japanese].

(3)D.S.Wood, M.Farrow and W.T.Burk : Proc. Conf. on Effects of Environment on Material Properties in Nuclear Systems, London/UK,1971 (British Nuclear Energy Society) paper 18.

(4)Y.Hosoi and S.Abe : Met. Trans. A, 6A, 1171 (1975).

(5)T.Nakanishi , N.Matsumoto and O.Kawada : Nihon-Kinzoku-Gakkai Shi (J. Jpn. Inst. Met.), 41, 263 (1977) [in Japanese].

(6)H.E.McCoy, Jr. : ORNL/TM-6822 (1979).

(7)K.Mino : Doctoral Thesis, Tokyo Institute of Technology (1981) [in Japanese].

(8)F.Schubert et al. : Nucl. Technol., 66, 227 (1984).

(9)K.S.Lee : ibid., 66, 241 (1984).

(10)T.Tanabe et al. : ibid., 66, 260 (1984).

(11)Y.Kurata, Y.Ogawa and T.Kondo :ibid., 66, 250(1984).

(12)Y.Ogawa, Y.Kurata , T.Suzuki, H.Nakajima and T.Kondo : Nihon-Genshiryoku-Gakkai Shi (J. At. Energy Soc. Japan), 36, 967 (1994) [in Japanese].

(13)HTTR Designing Laboratory, Department of Fuels and Materials Research and Department of High-Temperature Engineering : JAERI-M 89-005 (1989) [in Japanese].

(14)K.Hada, Y.Motoki and O.Baba : JAERI-M 90-148(1990) [in Japanese].

(15)M.Shindo and T.Kondo : Proc. Conf. on Gas-Cooled Reactors Today, Bristol/UK, 1982(British Nuclear Energy Society) Vol.2, p.179.

(16)Y.Ogawa and T.Kondo : JAERI-M 8801 (1980) [in Japanese].

(17)S.Yokoi, Y.Monma, T.Kondo, Y.Ogawa and Y.Kurata : JAERI-M 83-138

(1983) [in Japanese].

(18)Y.Kurata and H.Nakajima : JAERI-Research 94-004 (1994) [in Japanese].

(19)F.H.Norton : The Creep of Steel at High Temperature, McGraw-Hill, New York,(1929).

(20)H.J.Frost and M.F.Ashby : Deformation Mechanism Maps, Pergamon Press, London, (1982).

(21)D.Sidey and B.Wilshire : Met. Sci. J., 3, 56 (1969).

(22)A.J.Reynolds, B.L.Averbach and M.Cohen : Acta Mettall., 5, 29 (1957).

(23)F.C.Monkman and N.J.Grant : Proc. ASTM, 56, 593 (1956).

(24)R.Viswanathan : Damage Mechanism and Life Assessment of High-Temperature Components, ASM International, Metals Park, Ohio, (1989).

(25)VAMAS Data Evaluation Committee : Study on Standardization of Creep-Rupture Data Evaluation of Metals, The Iron and Steel Institute of Japan, (1994) [in Japanese].

(26)Y.Kurata, Y.Ogawa and H.Nakajima : Tetsu-to-Hagane (J. Iron Steel Inst. Jpn.), 74, 380 (1988) [in Japanese].

(27)idem. : ibid., 74, 2185 (1988) [in Japanese].

(28)M.Schutze and B.Glaser : Proc. Conf. Aspects of High Temperature Deformation and Fracture in Crystalline Materials, Nagoya, Vol.2, p.561 (1993), Jpn. Inst. Metals.

(29)S.Kihara, J.B.Newkirk, A.Ohtomo and Y.Saiga : Met. Trans.A, 11A, 1019 (1980).

(30)G.P.Sabol and R.Stickler : Phys. Stat. Sol., 35, 11(1969).

Table 1 Chemical composition of Hastelloy XR (mass %)

	Cr	Fe	C	Si	Co	Mn	B
Hastelloy X (ASTM B435)	20.5～23.0	17.0～20.0	0.05～0.15	max. 1.00	0.5～2.5	max. 1.00	—
Hastelloy XR	21.90	18.23	0.07	0.27	0.04	0.88	0.0003
	Mo	P	S	W	Al	Ti	Ni
Hastelloy X (ASTM B435)	8.0～10.0	max. 0.04	0.030	0.2～1.0	—	—	Remainder
Hastelloy XR	9.13	0.005	0.005	0.47	0.03	0.02	Remainder

Table 2 Impurity levels of JAERI Type B helium (vol ppm)

H_2	H_2O	CO	CO_2	CH_4
200～210	0.8～1.2	100～110	2～3	5～6

Table 3 Creep properties of Hastelloy XR at 800℃ in JAERI Type B helium

Stress (MPa)	Time to Rupture (h)	Rupture Elongation (%)	Reduction of area (%)	Steady-state creep rate (%/h)	Time to 1% strain (h)	Time to onset of tertiary creep (h)
98.1	104.4	41.3	36.1	1.06E-01	8	35
78.5	298.5	31.2	23.7	4.20E-02	41	105
60.8	980.7	18.0	16.0	1.63E-02	135	580
51.0	3706.8	16.0	13.6	2.40E-03	360	2180
47.1	11485.8	26.0	24.2	1.18E-03	430	6500
39.2	10944.1	32.0	36.0	1.35E-03	360	4050
36.3	33521.0	37.6	26.9	3.03E-04	470	11300

Table 4 Creep properties of Hastelloy XR at 900℃ in JAERI Type B helium

Stress (MPa)	Time to Rupture (h)	Rupture Elongation (%)	Reduction of area (%)	Steady-state creep rate (%/h)	Time to 1% strain (h)	Time to onset of tertiary creep (h)
58.8	62.0	47.3	55.3	1.85E-01	4	30
51.0	160.7	55.3	44.2	1.24E-01	10	69
49.0	217.8	43.3	41.2	1.21E-01	18	110
44.1	283.7	50.0	37.1	9.50E-02	20	140
39.2	694.7	41.7	36.0	3.50E-02	48	360
34.3	1579.6	35.8	30.6	1.10E-02	130	860
29.4	3839.7	24.6	21.3	4.20E-03	210	2000
26.5	3999.7	22.0	17.8	2.86E-03	660	2400
23.5	7447.1	26.0	30.0	3.16E-03	360	4130
23.5	8149.9	30.7	25.0	2.16E-03	470	3100
19.6	7936.6	34.0	30.0	1.80E-03	770	3300
13.7	48587.5	33.1	23.7	3.30E-04	550	20650

Table 5 Creep properties of Hastelloy XR at 1000℃ in JAERI Type B helium

Stress (MPa)	Time to Rupture (h)	Rupture Elongation (%)	Reduction of area (%)	Steady-state creep rate (%/h)	Time to 1% strain (h)	Time to onset of tertiary creep (h)
24.5	196.2	55.0	43.2	1.50E-01	22	112
19.6	410.6	42.3	33.4	6.72E-02	36	212
15.7	699.2	41.0	32.2	2.70E-02	43	350
12.7	2498.3	35.3	24.6	7.90E-03	250	1380
9.8	2247.3	45.3	35.5	2.90E-03	510	1100
9.8	8111.1	34.0	22.0	2.00E-03	1160	2650
6.9	13014.0	32.0	26.3	5.95E-04	1640	3650

Table 6 Comparison of standard TTP(time-temperature parameter) fit for rupture lives of Hastelloy XR

Degree of Polynomals	SEE(standard error of estimate)	
	Larson-Miller Parameter	Orr-Sherby-Dorn Parameter
1	0.223	0.278
2	0.160	0.173
3	0.164	0.175
4	0.159	0.171
5	0.156	0.168

Table 7 Comparison of SEE(standard error of estimate) and RMS(root mean squares) values estimated by Larson-Miller parameter fit using data below 5,000h for Hastelloy XR

Degree of polynomals	SEE	RMS
2	0.140	0.241

Table 8 Carbon analysis results on the specimens of Hastelloy XR ruptured in JAERI Type B helium

Temperature (℃)	Stress (MPa)	Time to rupture (h)	Carbon content (mass %)	
			Rupture region	φ8mm region
800	98.1	104.4	0.074	0.072
800	78.5	298.5	0.082	0.072
800	60.8	980.7	0.077	0.072
800	51.0	3706.8	0.077	0.072
800	47.1	11485.8	0.080	0.071
800	36.3	33521.0	0.104	0.072
900	49.0	217.8	0.080	0.073
900	44.1	283.7	0.092	0.072
900	39.2	694.7	0.080	0.075
900	26.5	3999.7	0.079	0.074
900	23.5	7447.1	0.103	0.069
900	13.7	48587.5	0.102	0.075
1000	24.5	196.2	0.094	0.073
1000	19.6	410.6	0.097	0.077
1000	15.7	699.2	0.093	0.073
1000	12.7	2498.3	0.108	0.076
1000	9.8	2247.3	0.123	0.075
1000	9.8	8111.1	0.153	0.073

Table 9 Quantitative analysis results of precipitates and matrix of Hastelloy XR ruptured in 13,014h at 1000℃ under 6.9MPa (mass %)

	Ni	Cr	Fe	Mo	Mn	W
Precipitate (Dark)	4.7	71.6	3.6	18.7	0.36	0.99
Precipitate (Bright)	20.2	16.1	6.4	53.8	0.16	3.3
Matrix	49.6	22.8	18.5	7.7	0.93	0.40

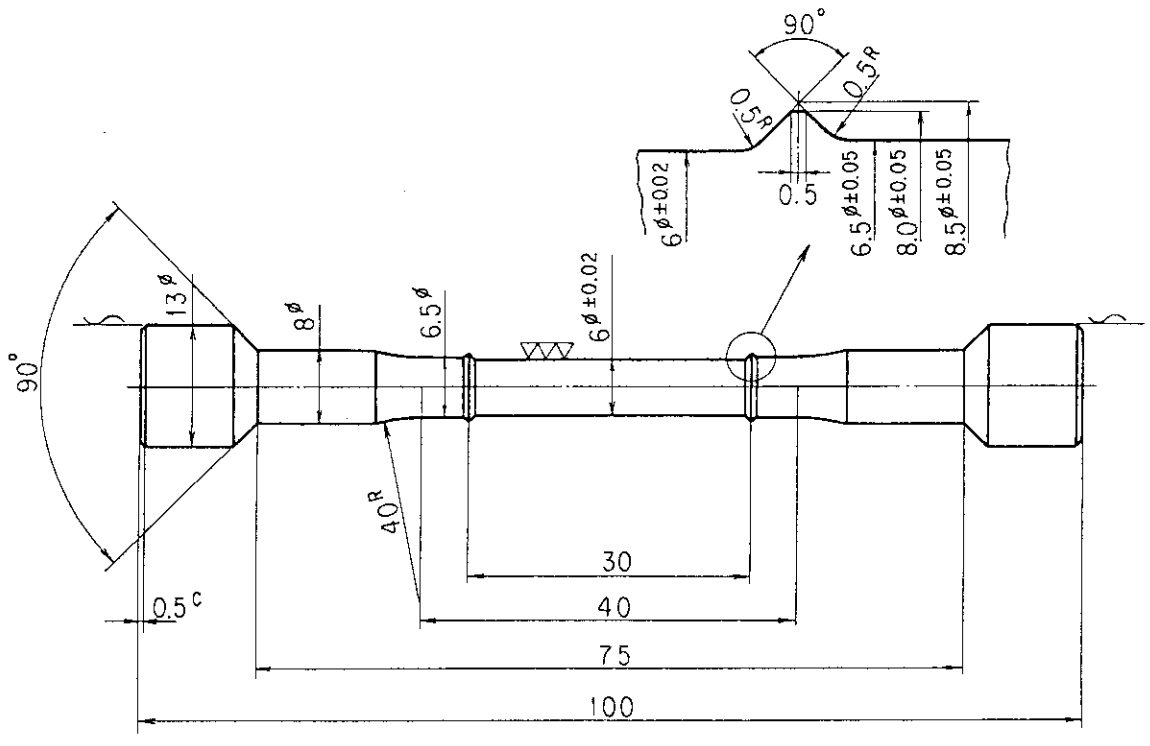

UNIT (mm)

Fig. 1 Geometry of specimen for creep test in helium environment.

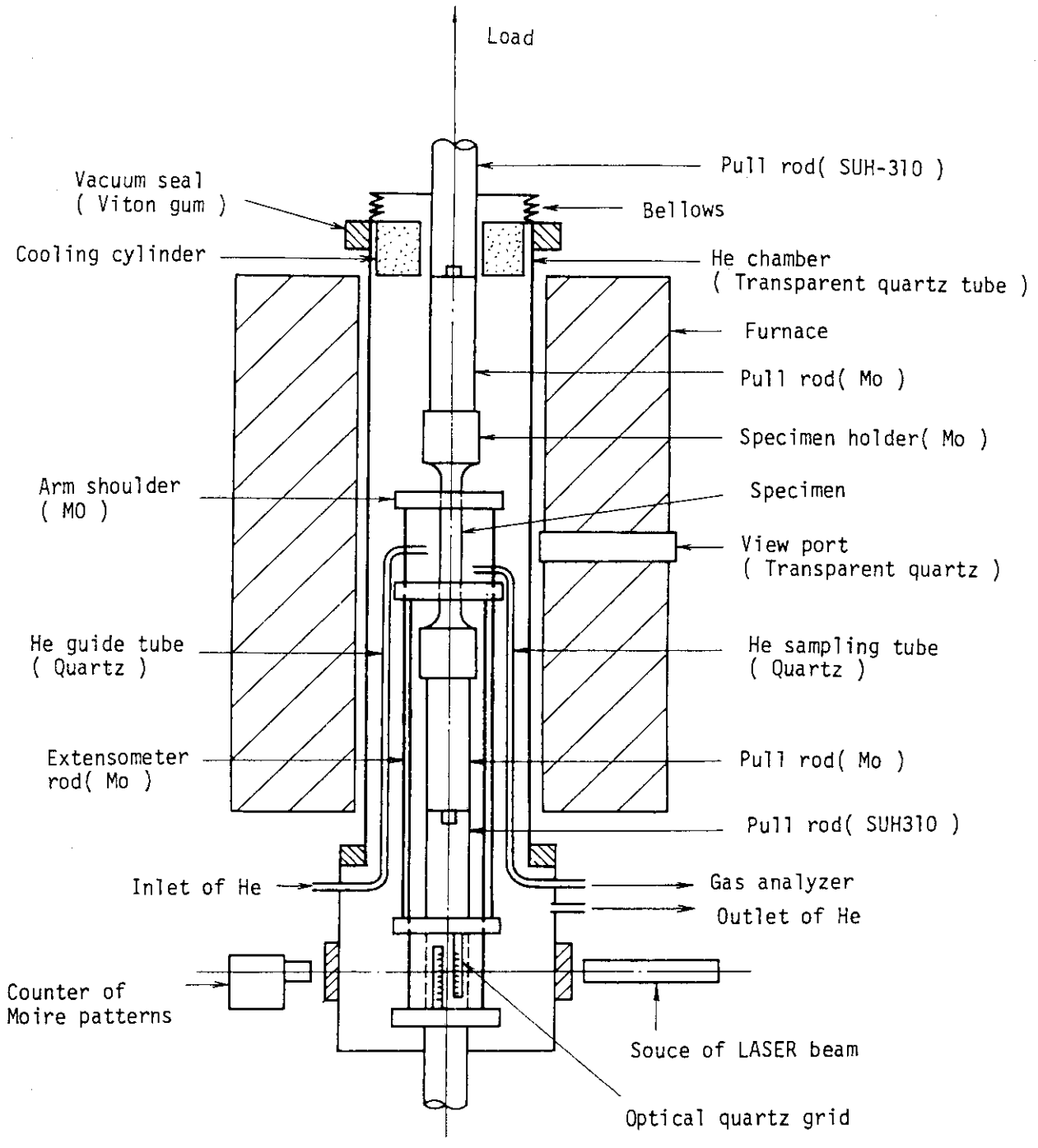

Fig. 2 Test section of creep testing machine for helium environment. Helium chamber is made of a transparent quartz tube. Displacement between two gauge points of the specimen is measured with a device for counting Moire patterns developed specially for this test.

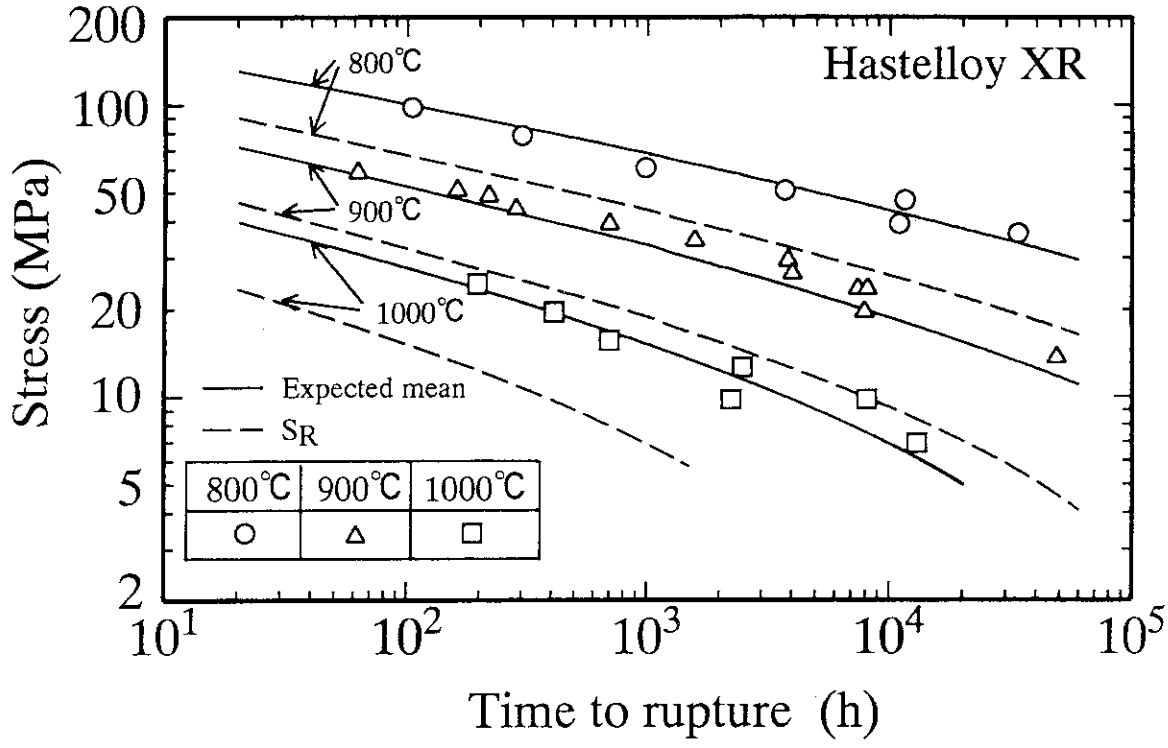

Fig. 3 Stress vs. time to rupture for Hastelloy XR in JAERI Type B helium. The solid lines are expected mean values, and the broken lines the design allowable creep-rupture stress(S_R) of the Design Allowable Limits[14].

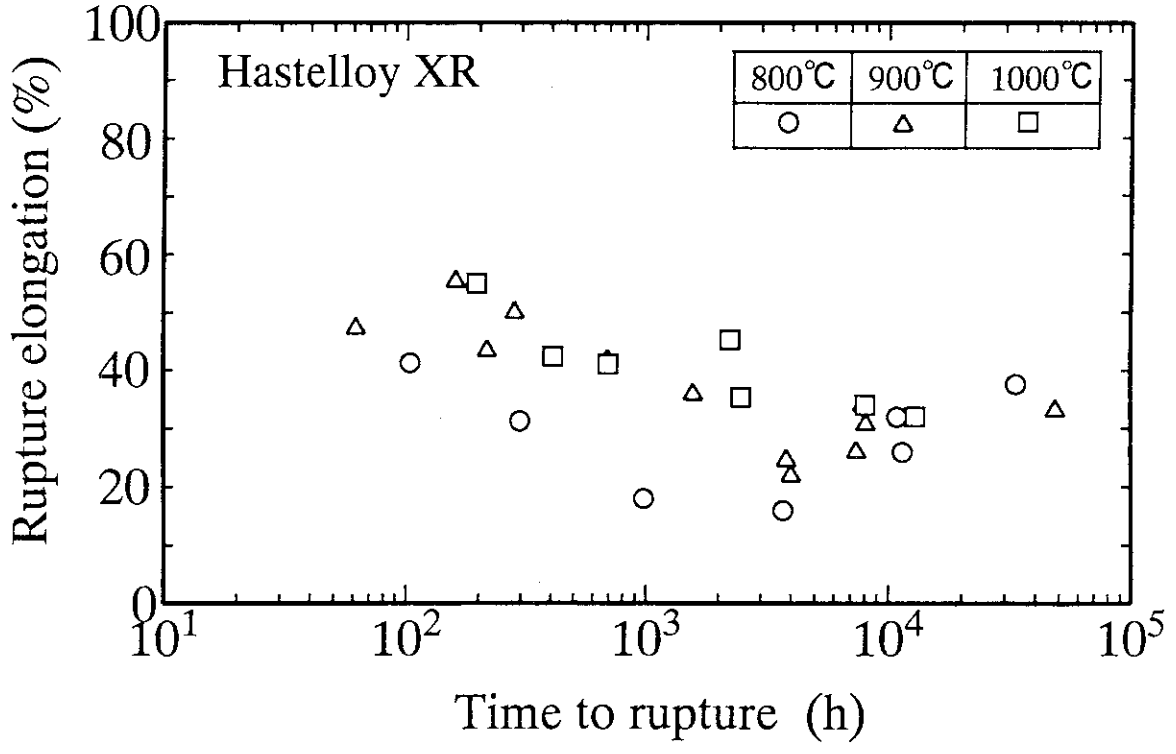

Fig. 4 Rupture elongation vs. time to rupture for Hastelloy XR in JAERI Type B helium.

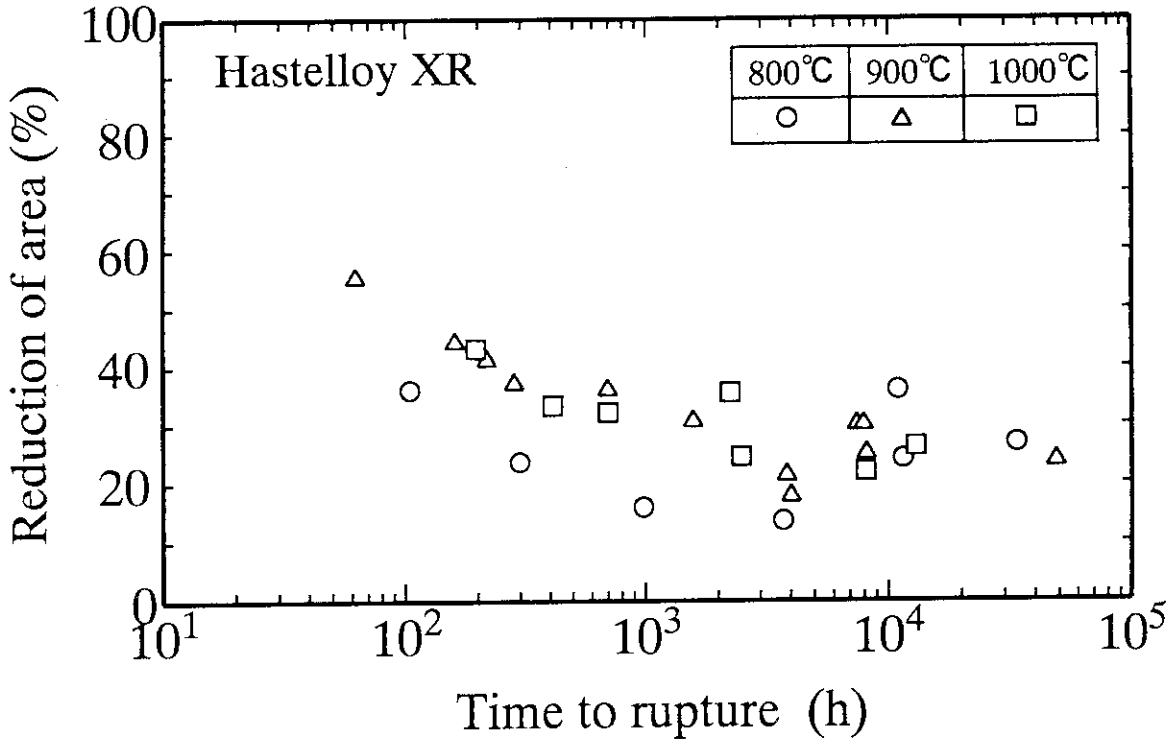

Fig. 5 Reduction of area vs. time to rupture for Hastelloy XR in JAERI Type B helium.

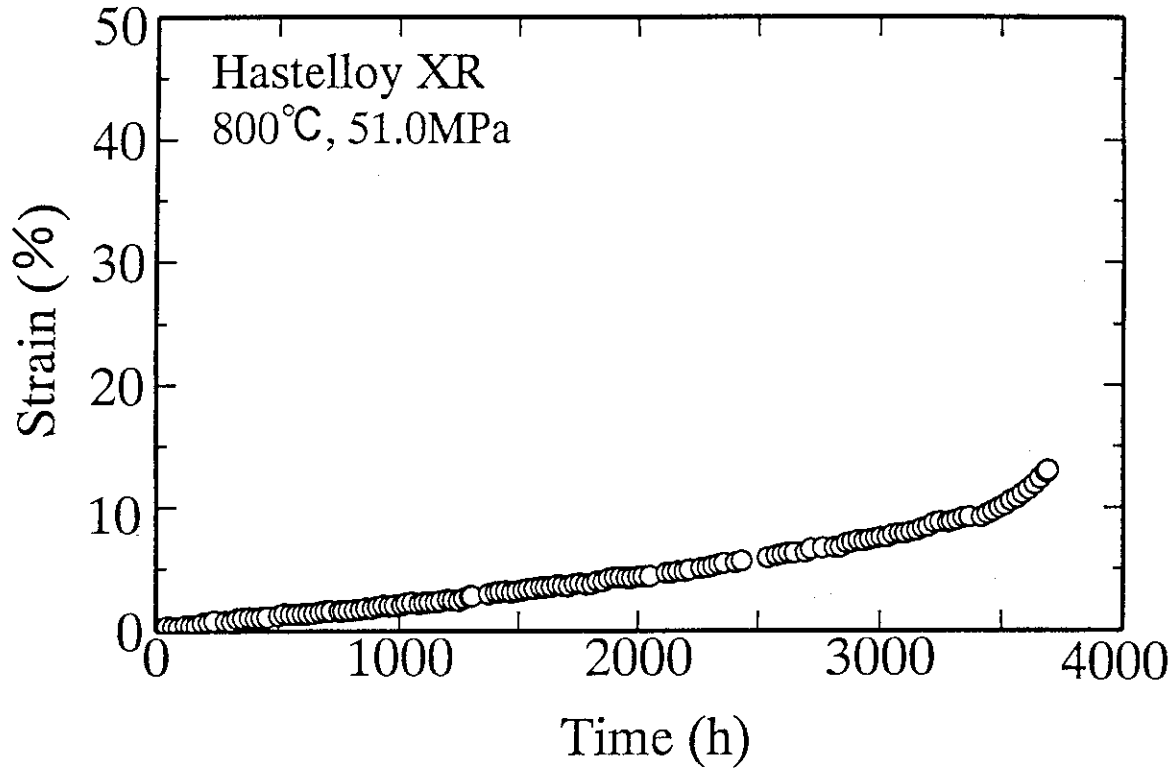

Fig. 6(a) Creep curve of Hastelloy XR tested at 800℃ under 51.0 MPa in JAERI Type B helium.

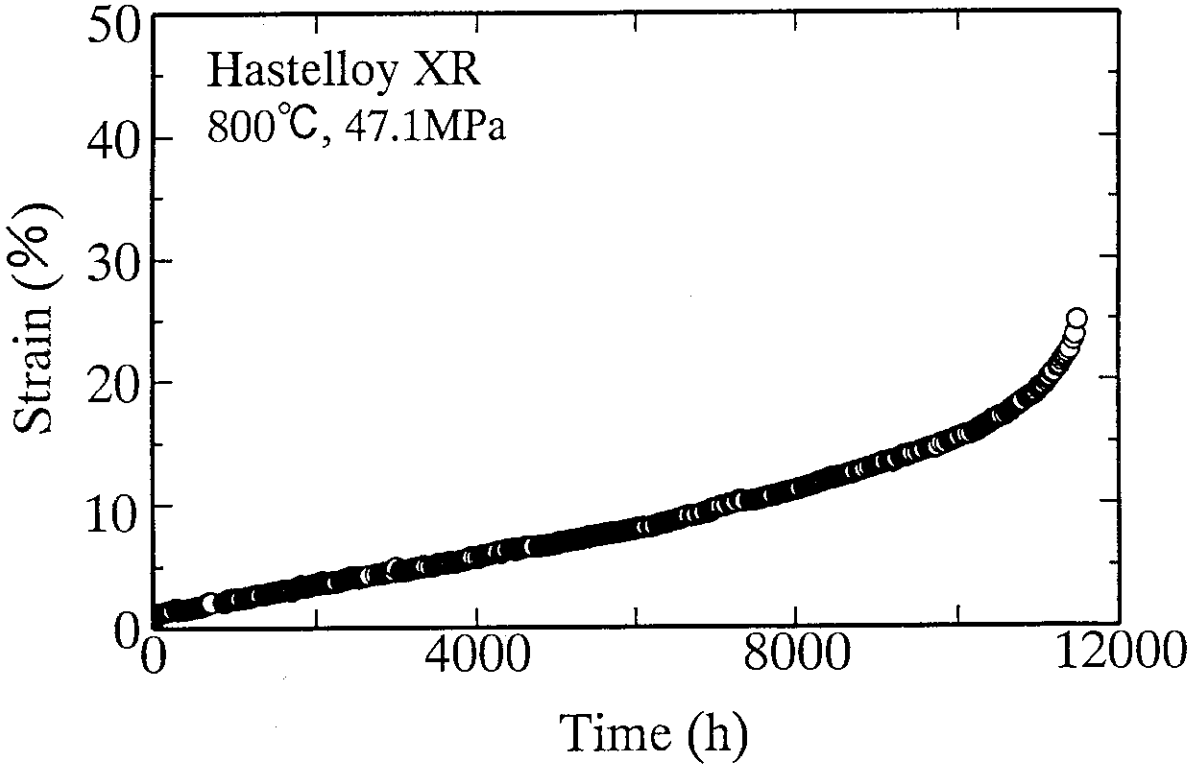

Fig. 6(b) Creep curve of Hastelloy XR etsted at 800℃ under 47.1 MPa in JAERI Type B helium.

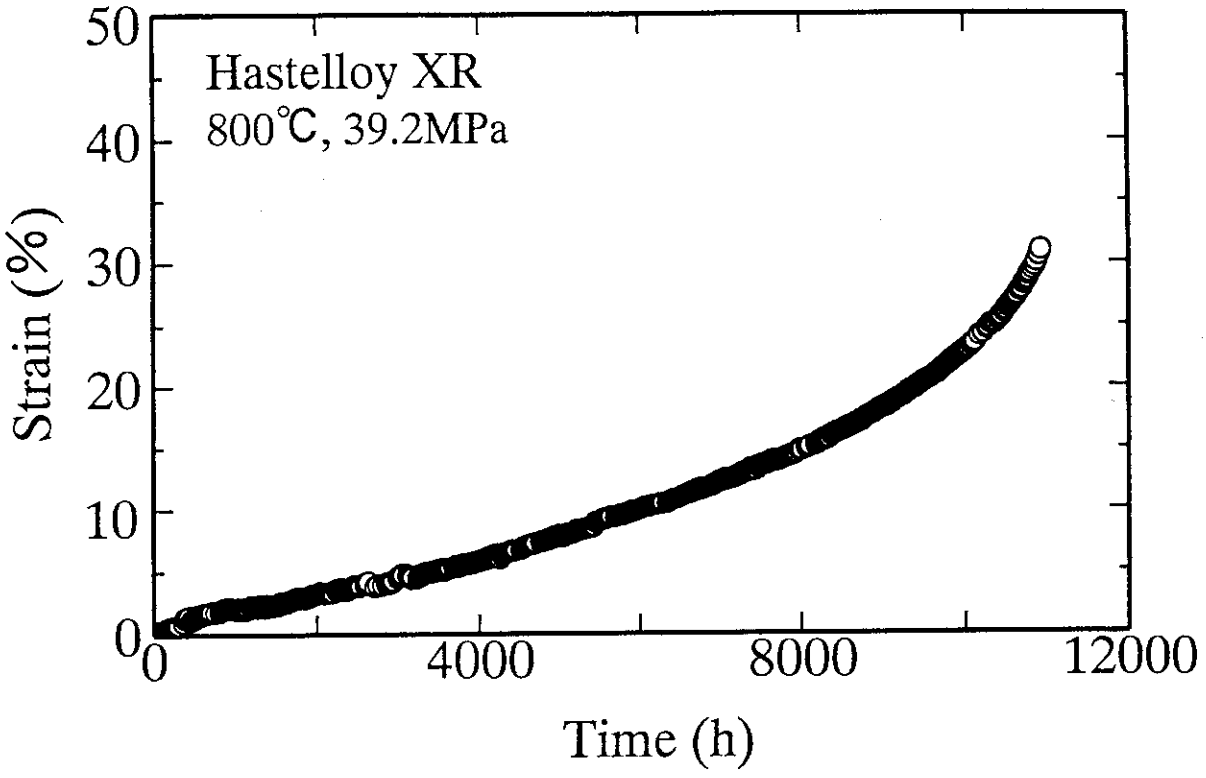

Fig. 6(c) Creep curve of Hastelloy XR tested at 800℃ under 39.2 MPa in JAERI Type B helium.

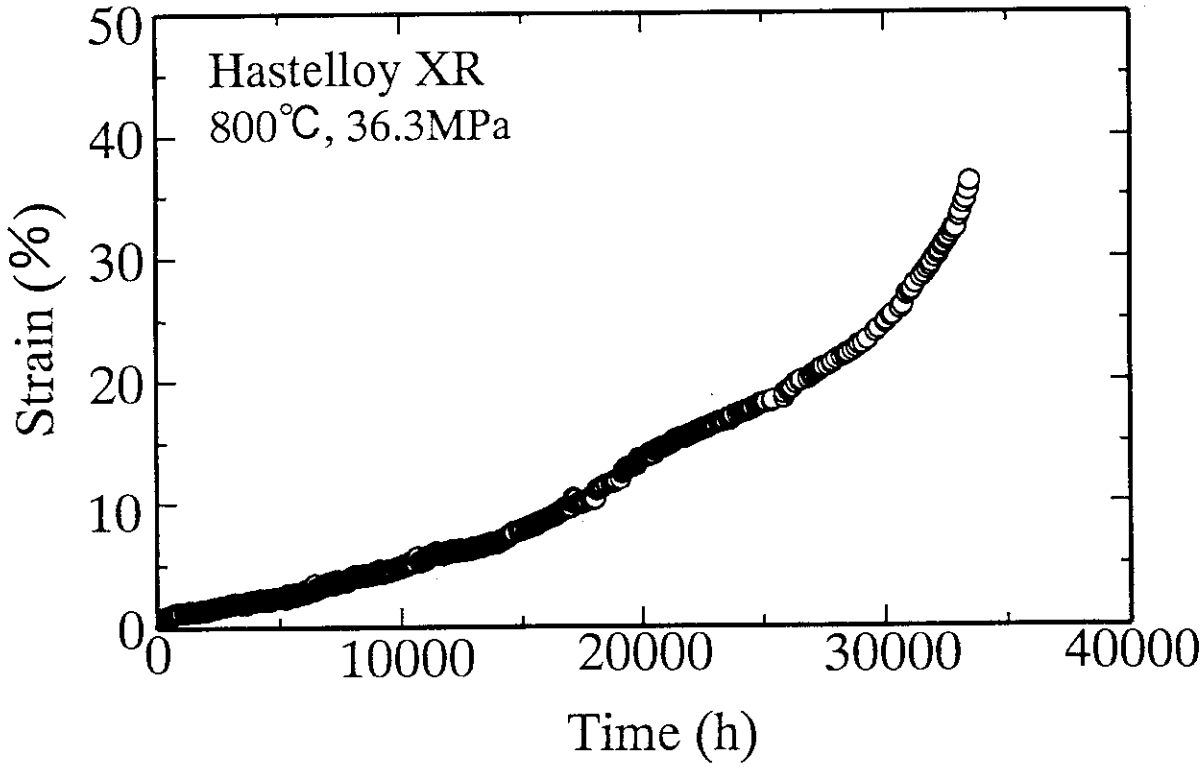

Fig. 6(d) Creep curve of Hastelloy XR tested at 800℃ under 36.3 MPa in JAERI Type B helium.

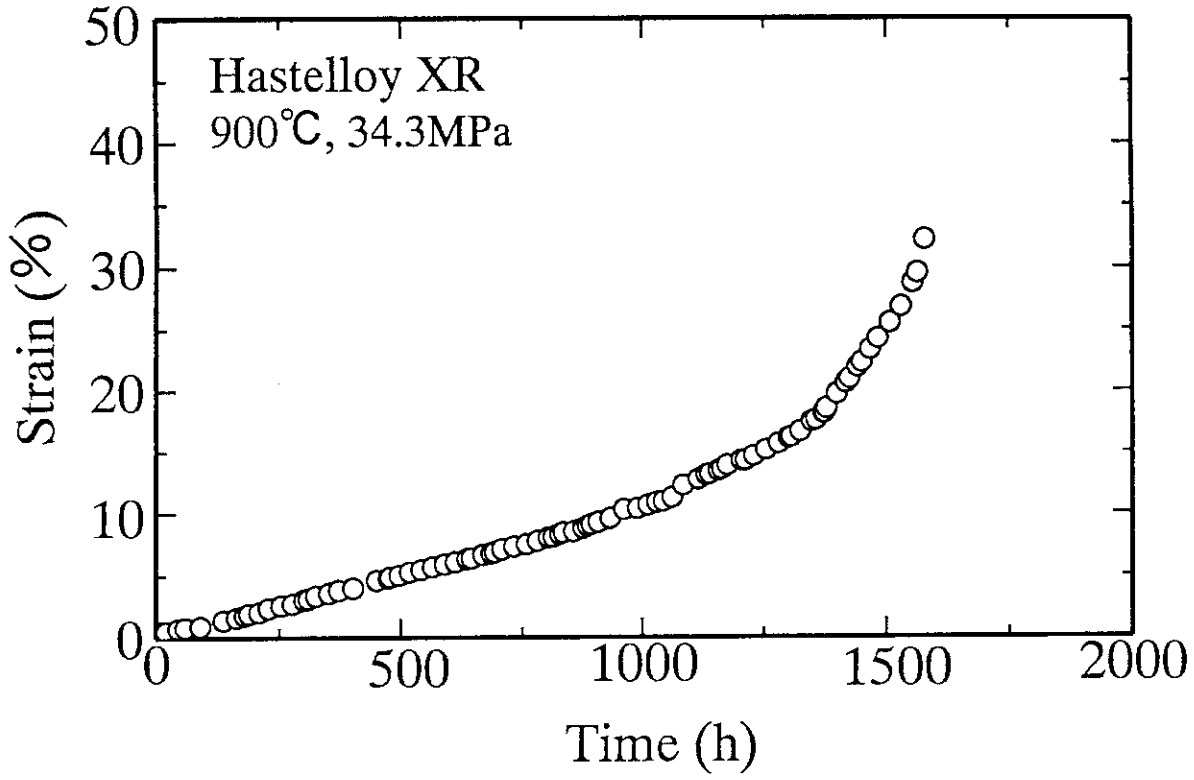

Fig. 7(a) Creep curve of Hastelloy XR tested at 900℃ under 34.3 MPa in JAERI Type B helium.

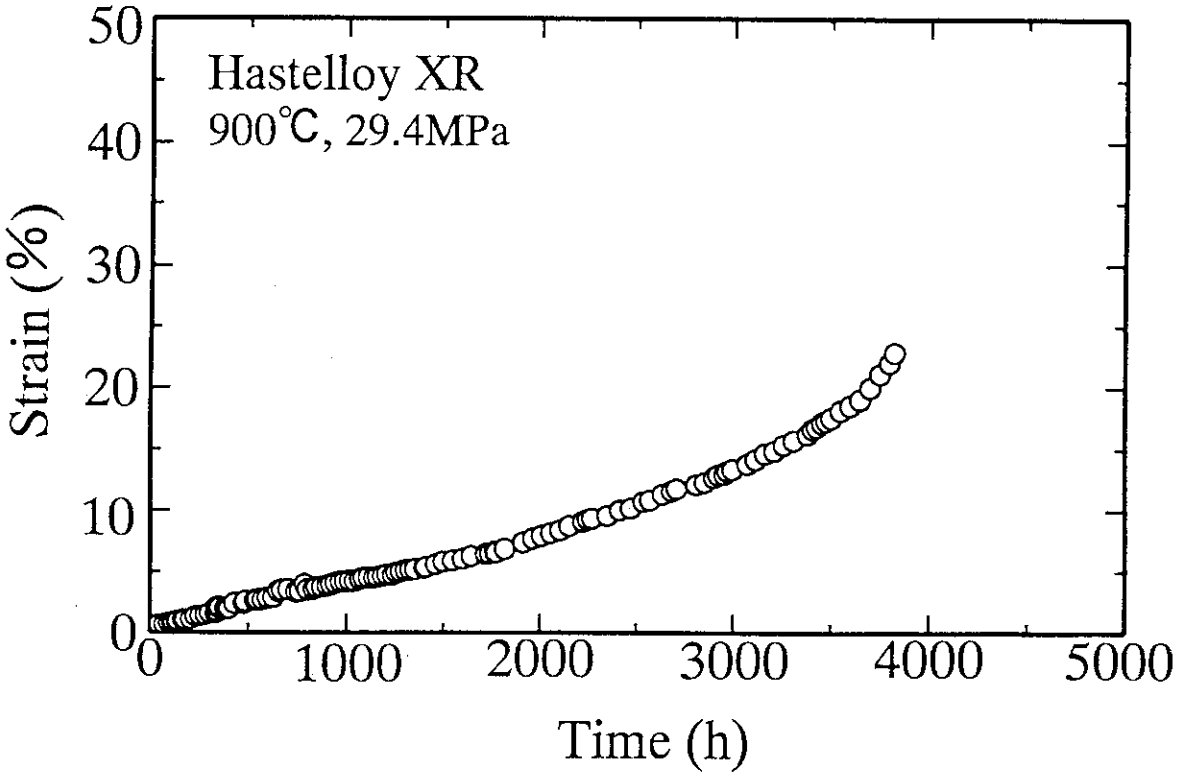

Fig. 7(b) Creep curve of Hastelloy XR tested at 900℃ under 29.4 MPa in JAERI Type B helium.

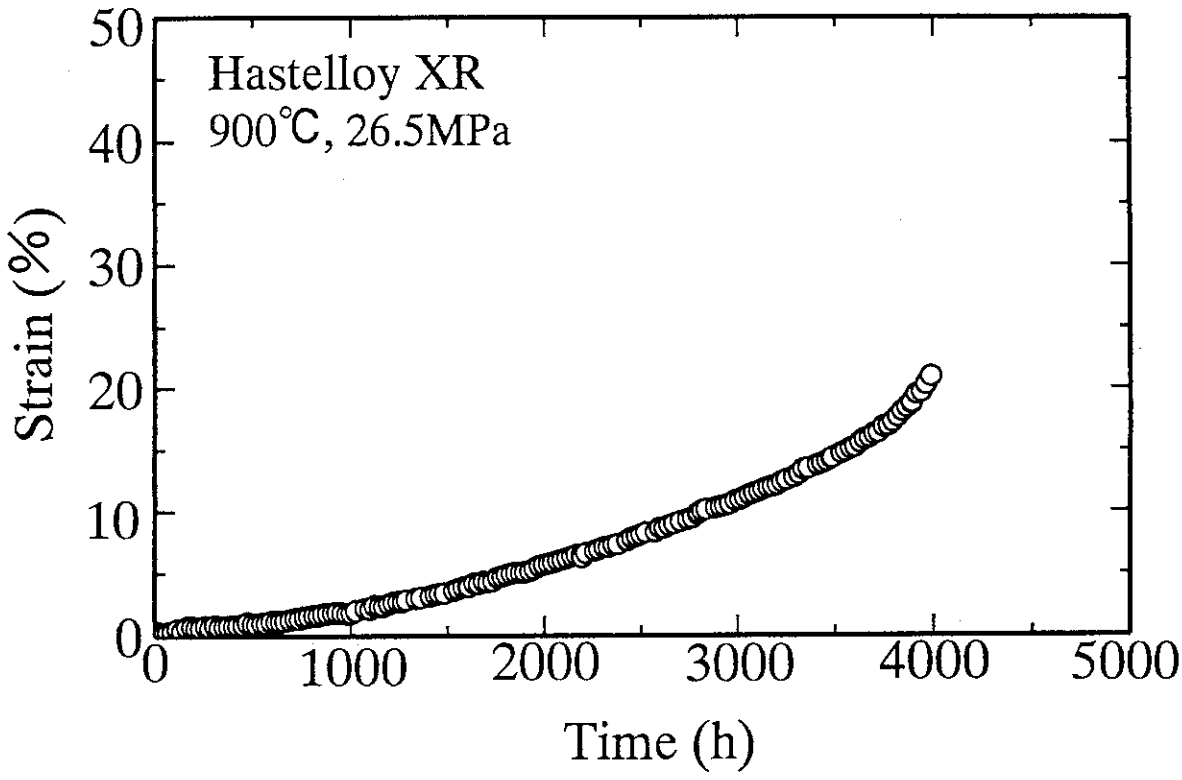

Fig. 7(c) Creep curve of Hastelloy XR tested at 900℃ under 26.5 MPa in JAERI Type B helium.

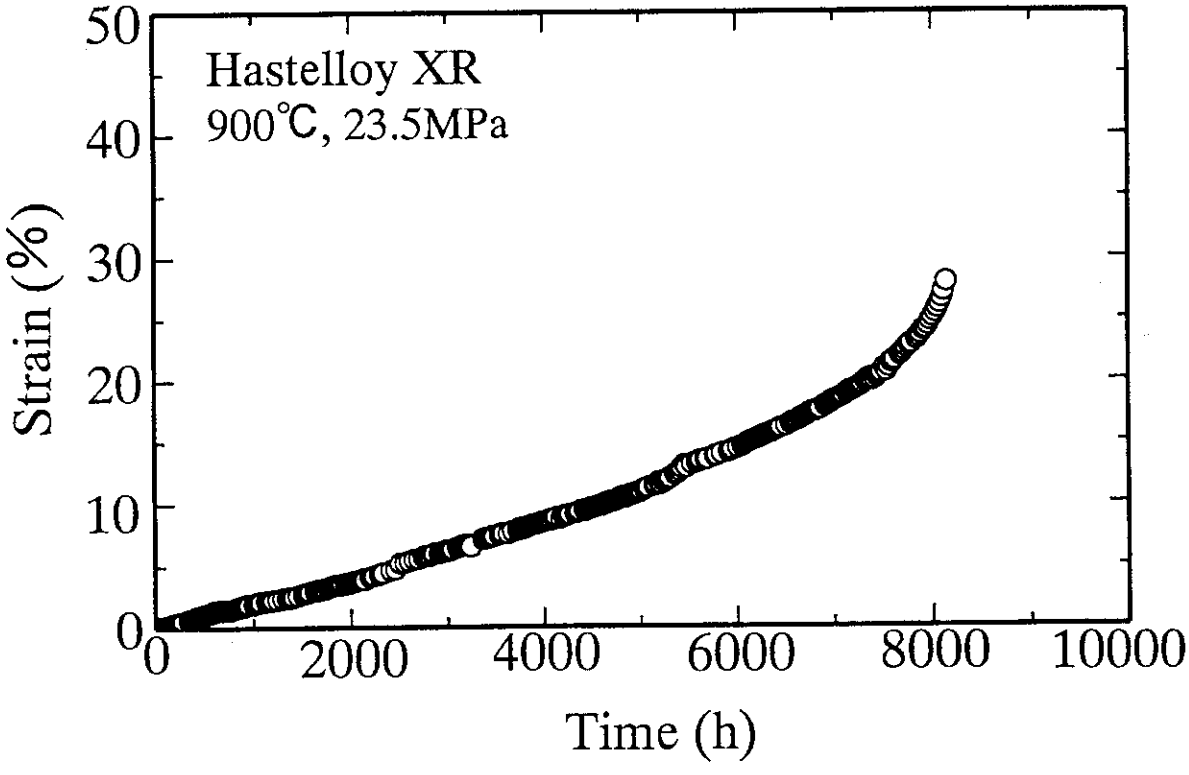

Fig. 7(d) Creep curve of Hastelloy XR tested at 900℃ under 23.5 MPa in JAERI Type B helium.

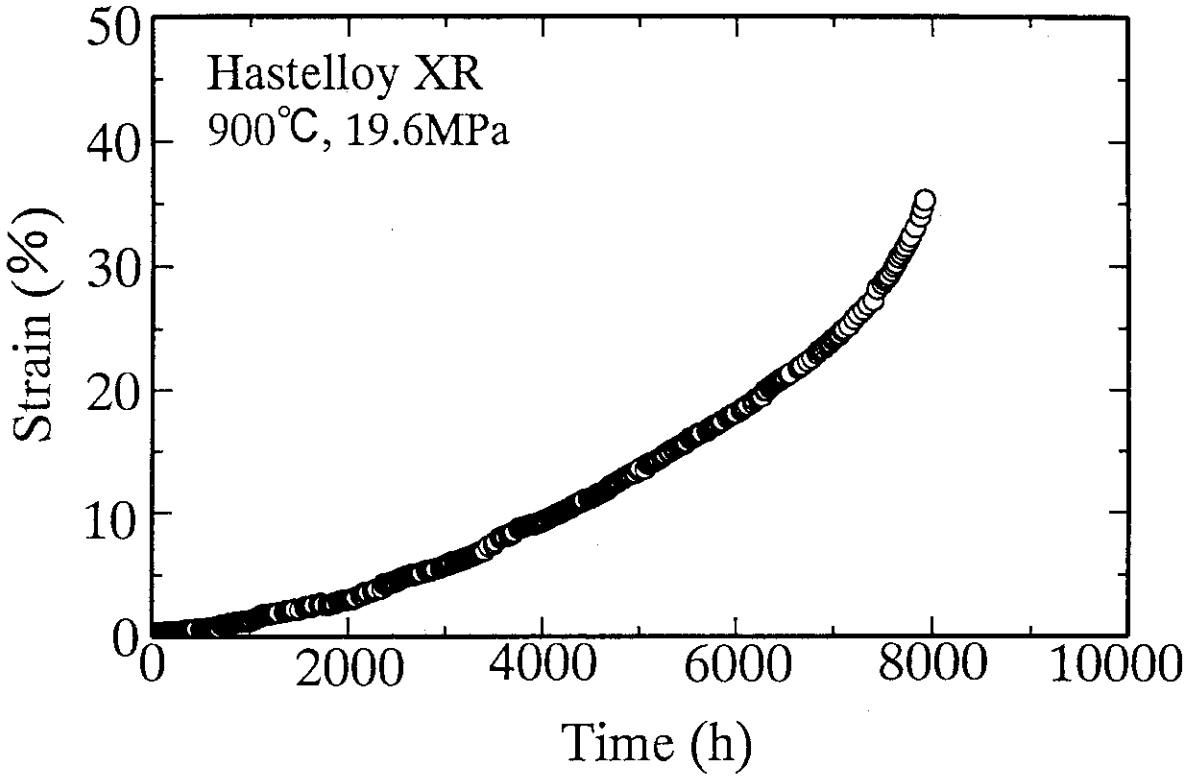

Fig. 7(e) Creep curve of Hastelloy XR tested at 900℃ under 19.6 MPa in JAERI Type B helium.

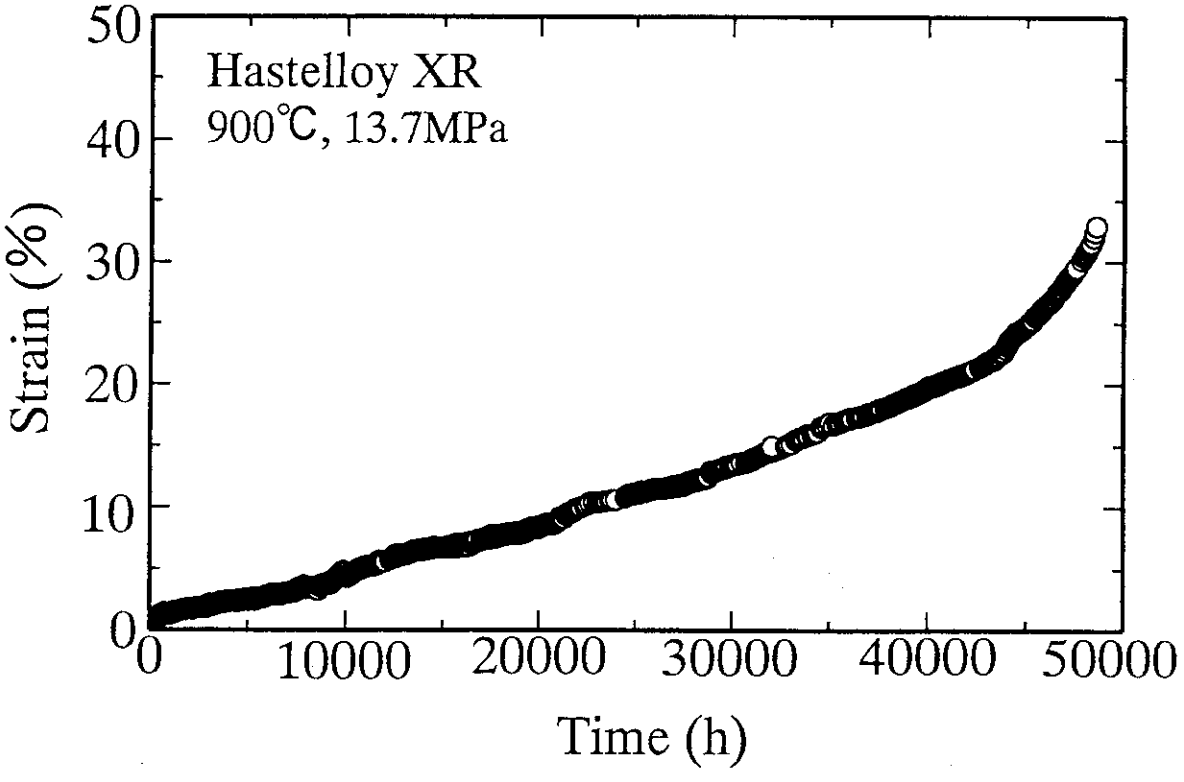

Fig. 7(f) Creep curve of Hastelloy XR tested at 900℃ under 13.7 MPa in JAERI Type B helium.

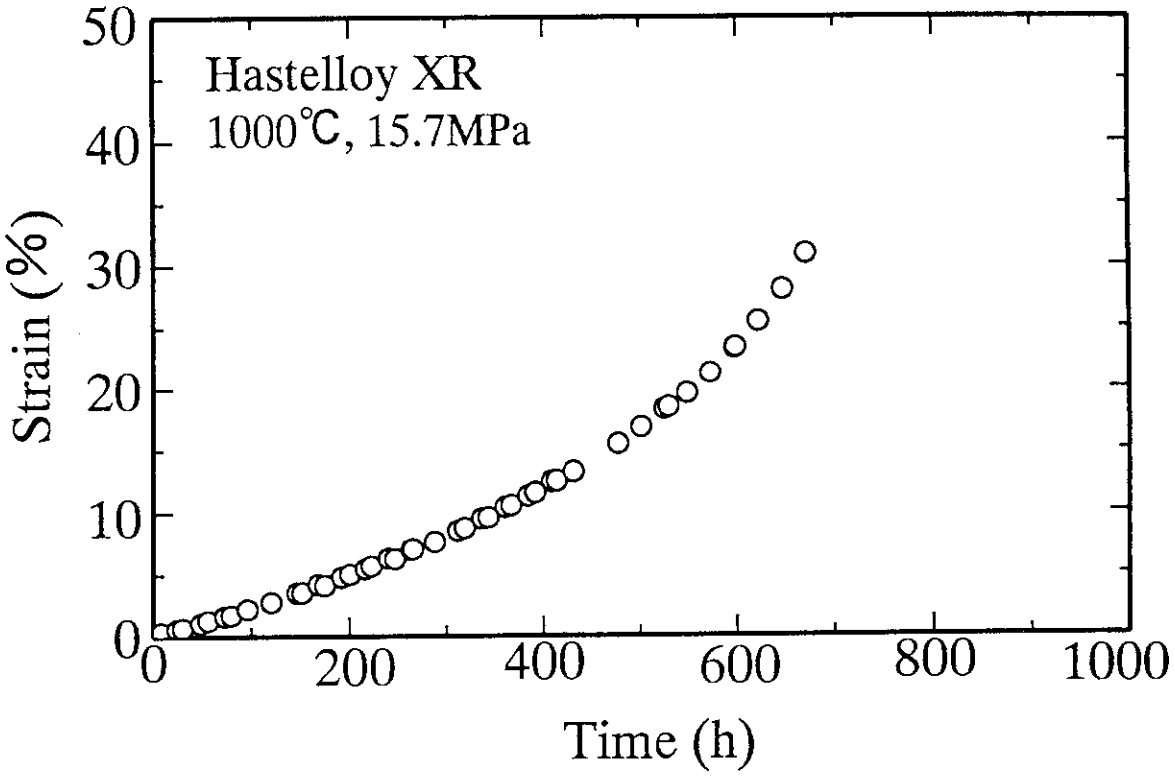

Fig. 8(a) Creep curve of Hastelloy XR tested at 1000℃ under 15.7 MPa in JAERI Type B helium.

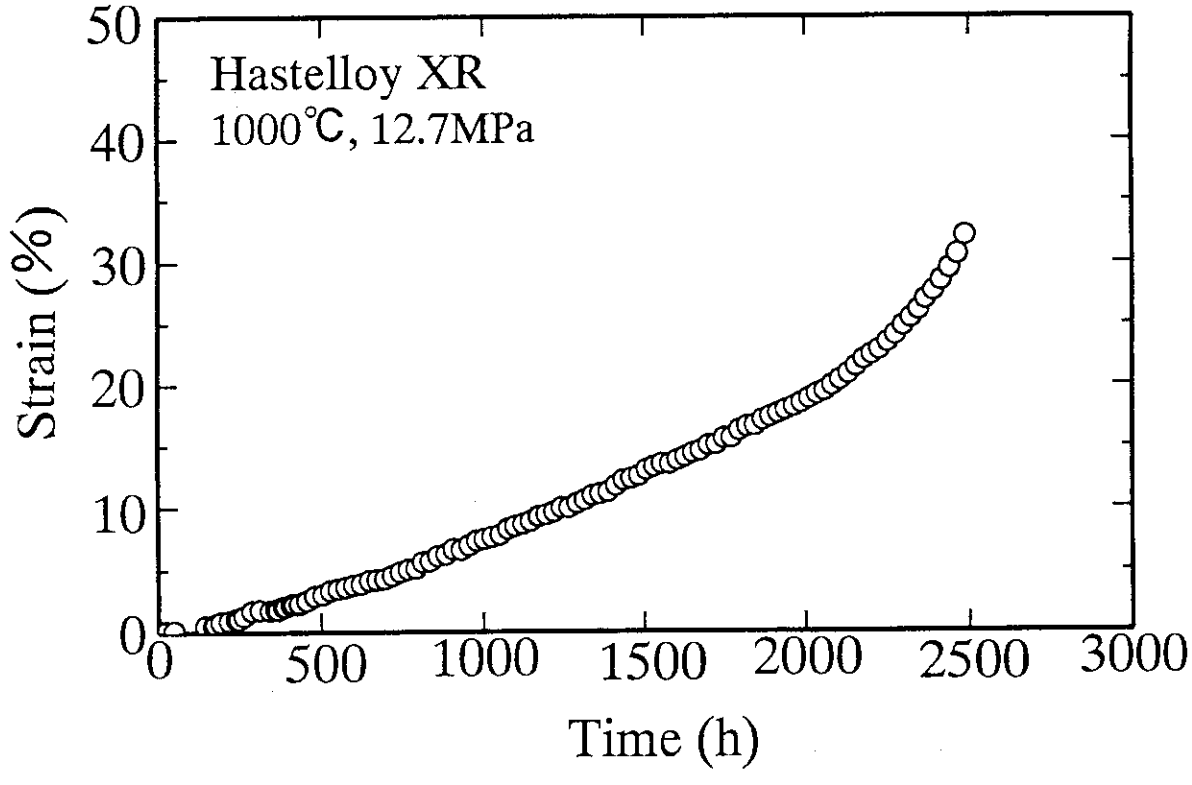

Fig. 8(b) Creep curve of Hastelloy XR tested at 1000℃ under 12.7 MPa in JAERI Type B helium.

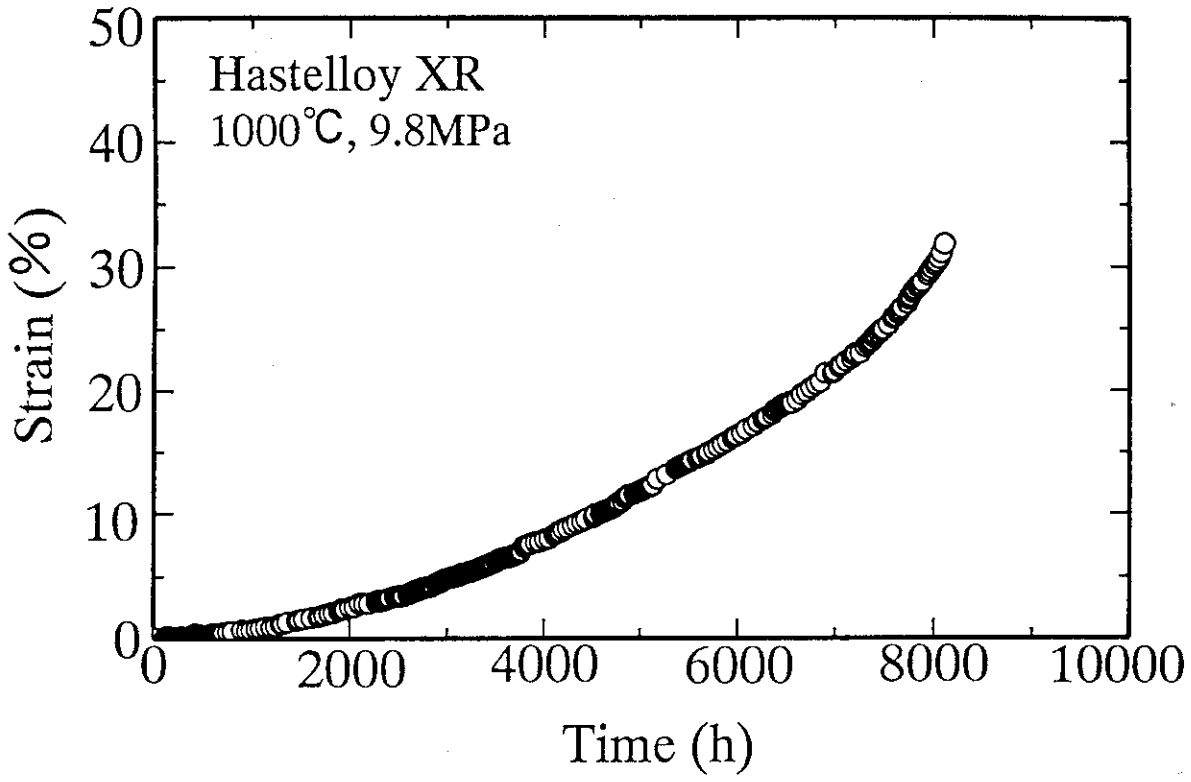

Fig. 8(c) Creep curve of Hastelloy XR tested at 1000℃ under 9.8 MPa in JAERI Type B helium.

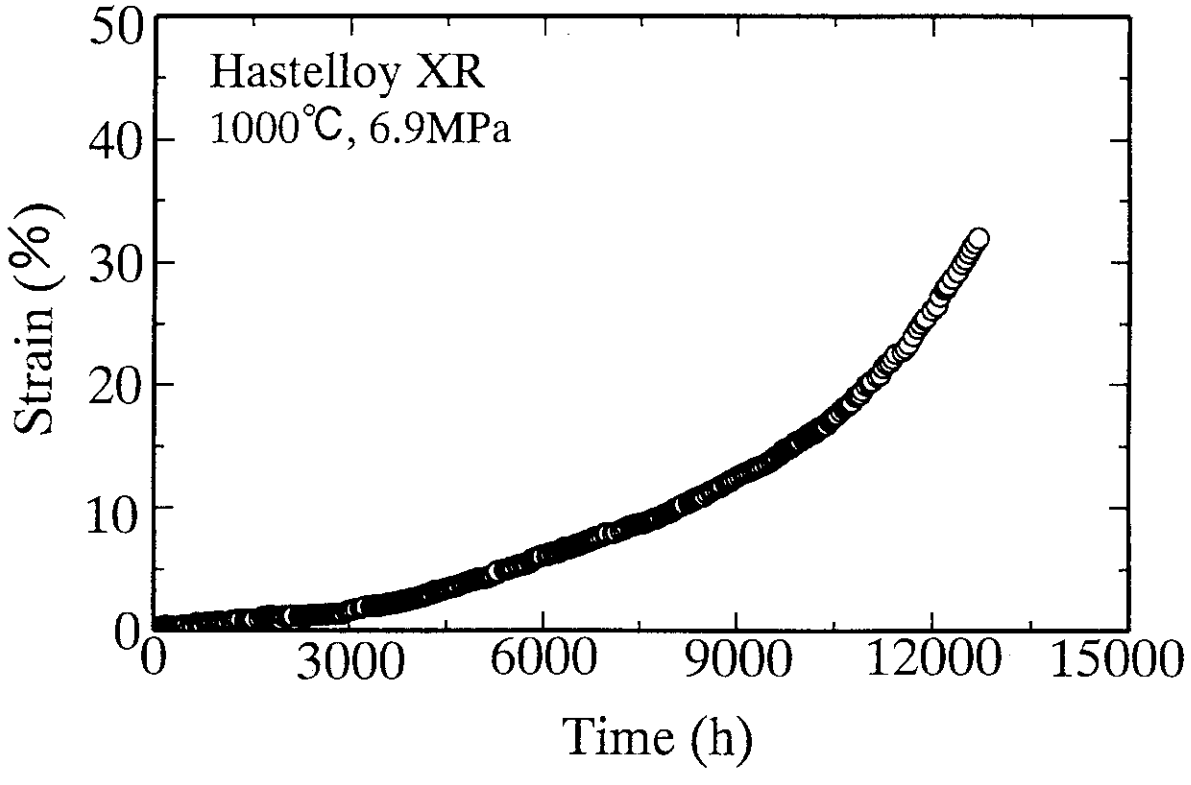

Fig. 8(d) Creep curve of Hastelloy XR tested at 1000℃ under 6.9 MPa in JAERI Type B helium.

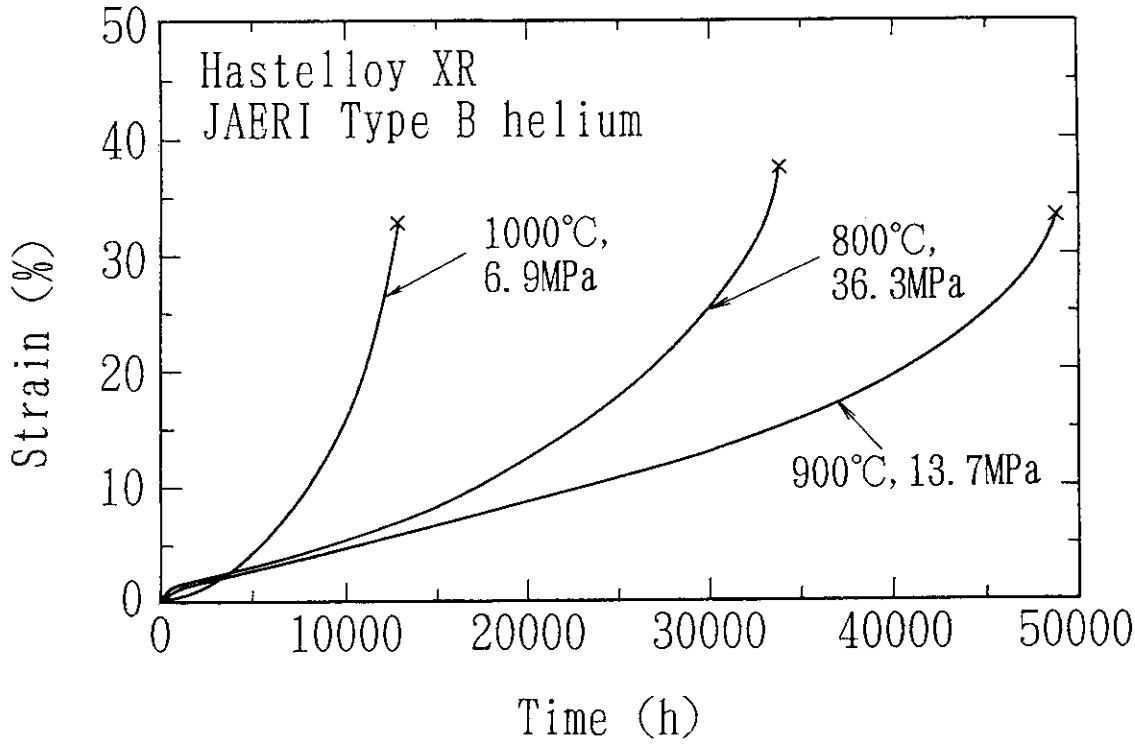

Fig. 9 Long-term creep curves of Hastelloy XR tested at 800,900 and 1000 ℃ in JAERI Type B helium.

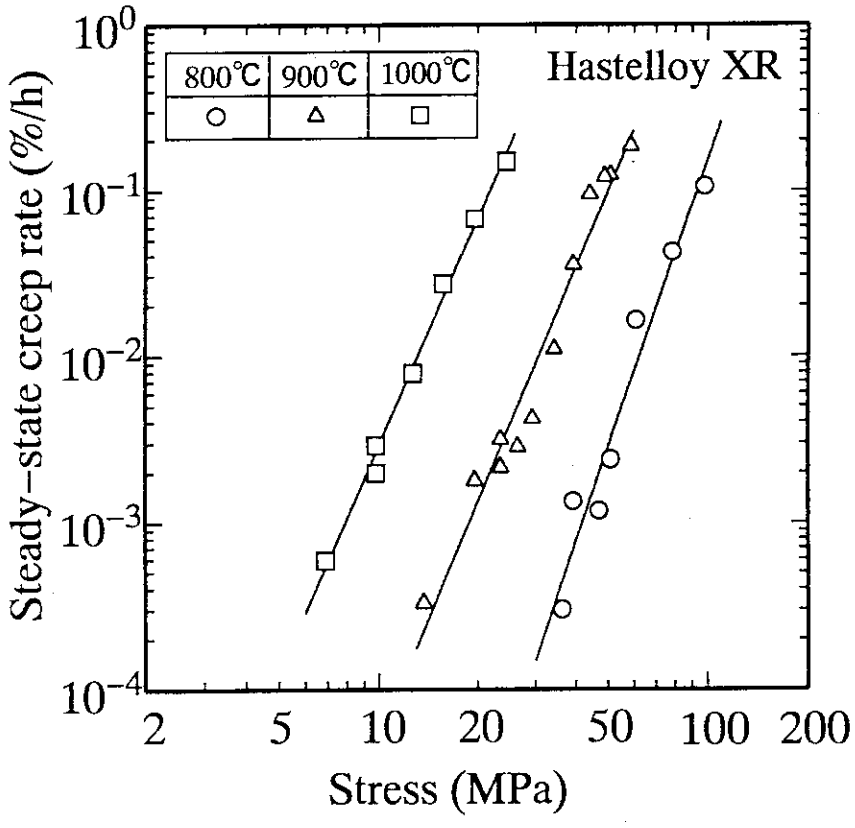

Fig. 10 Relationship between steady-state creep rate and stress for Hastelloy XR in JAERI Type B helium.

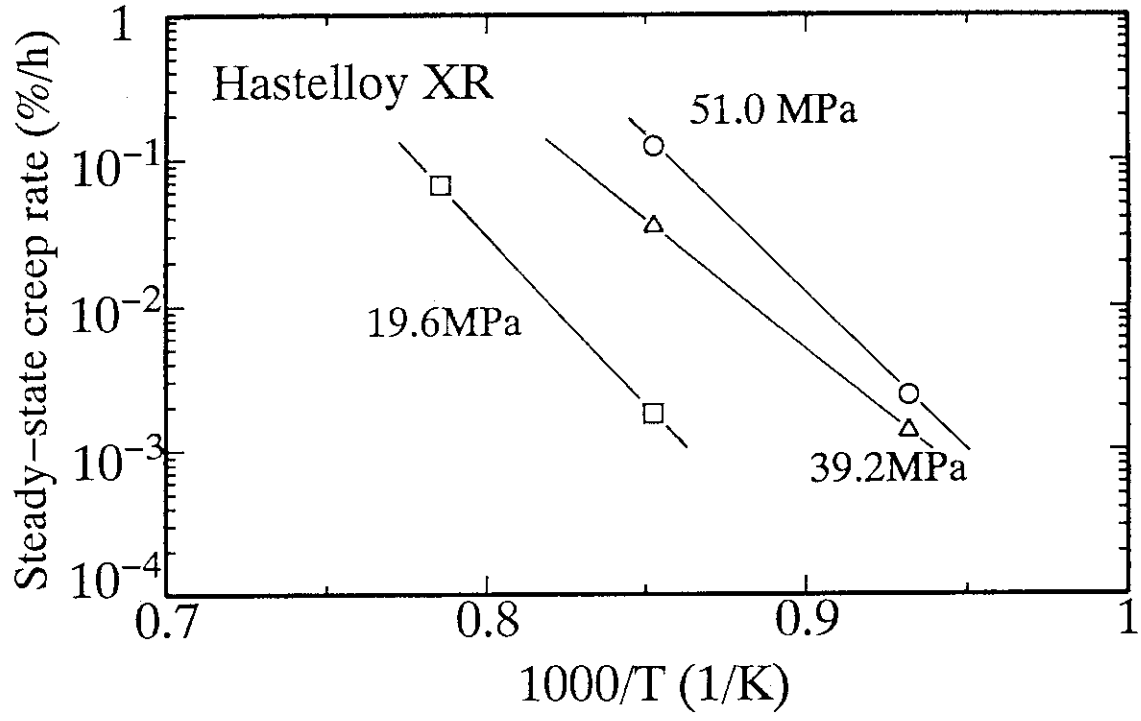

Fig. 11 Relationship between steady-state creep rate and the reciprocal of absolute temperature under constant stress for Hastelloy XR in JAERI Type B helium.

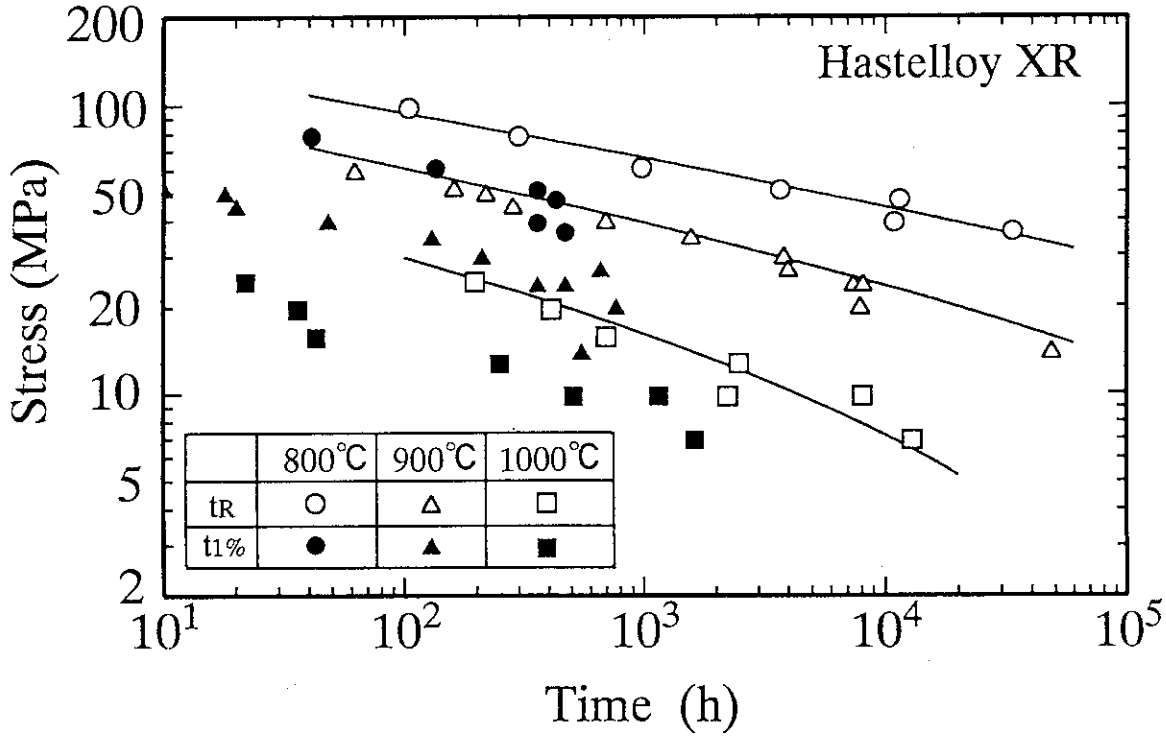

Fig. 12 Stress vs. time to 1% total strain($t_{1\%}$) and time to rupture (t_R) for Hastelloy XR tested at 800 and 1000℃ in JAERI Type B helium.

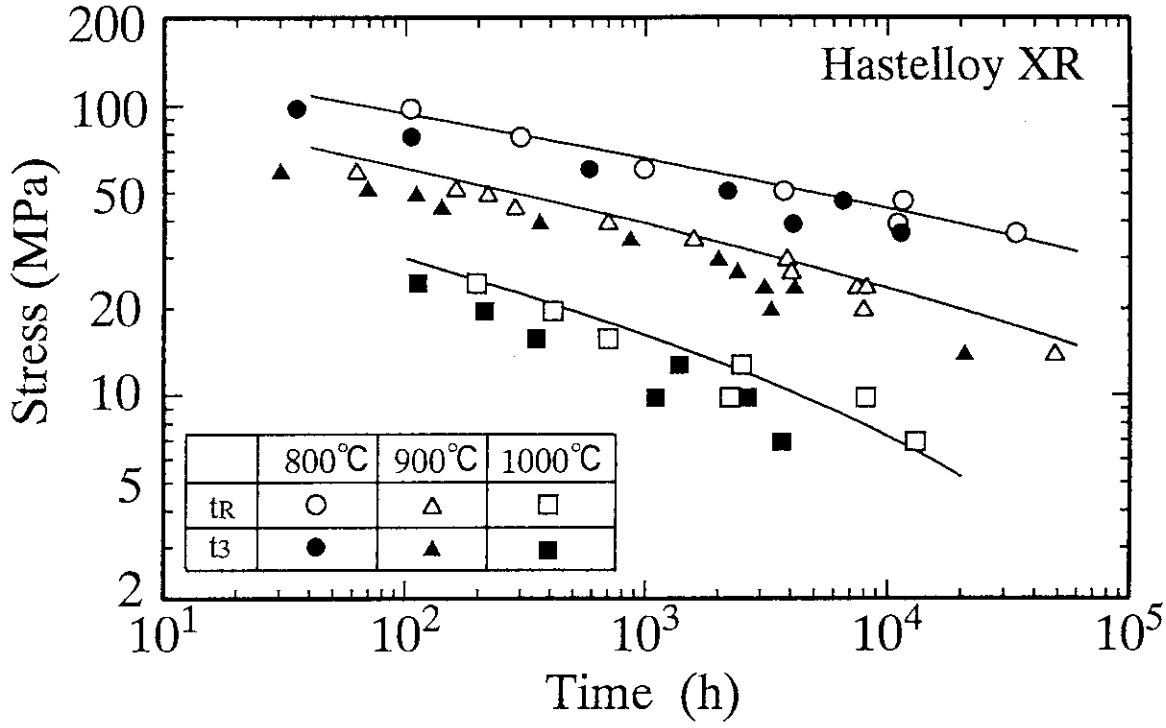

Fig. 13 Stress vs. time to onset of tertiary creep(t_3) and time to rupture(t_R) for Hastelloy XR tested at 800,900 and 1000℃ in JAERI Type B helium.

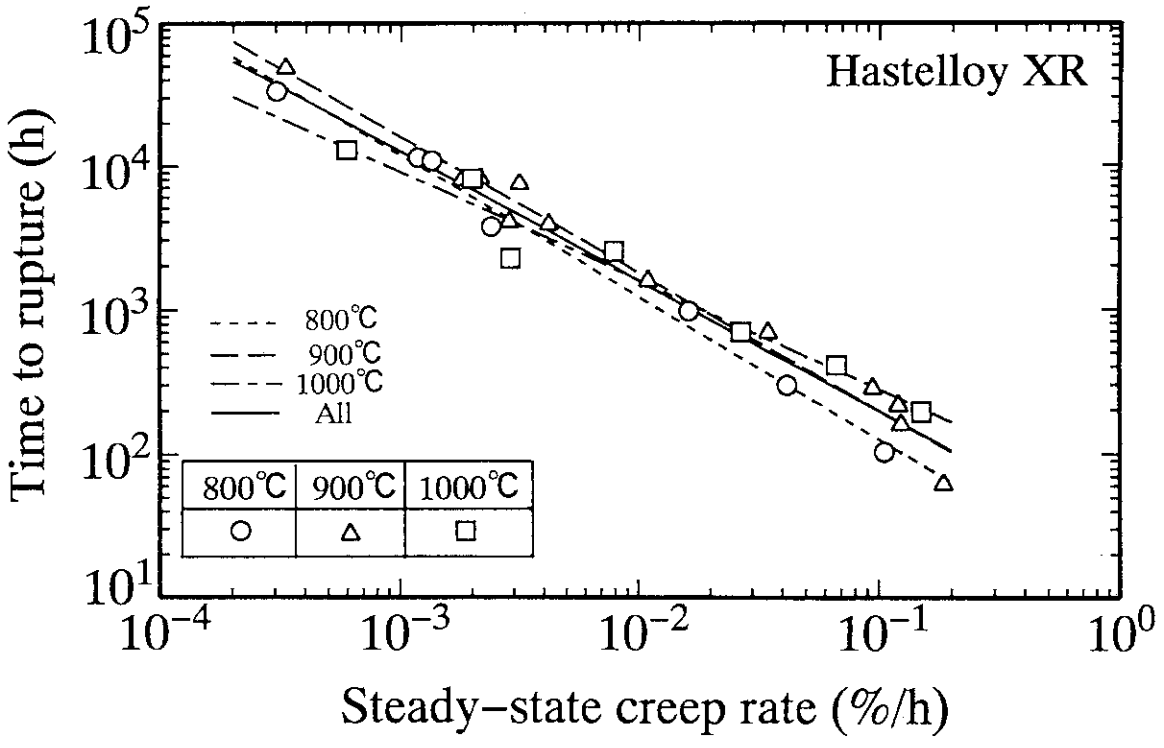

Fig. 14 Relationship between time to rupture and steady-state creep rate (Monkman-Grant relationship)for Hastelloy XR in JAERI Type B helium.

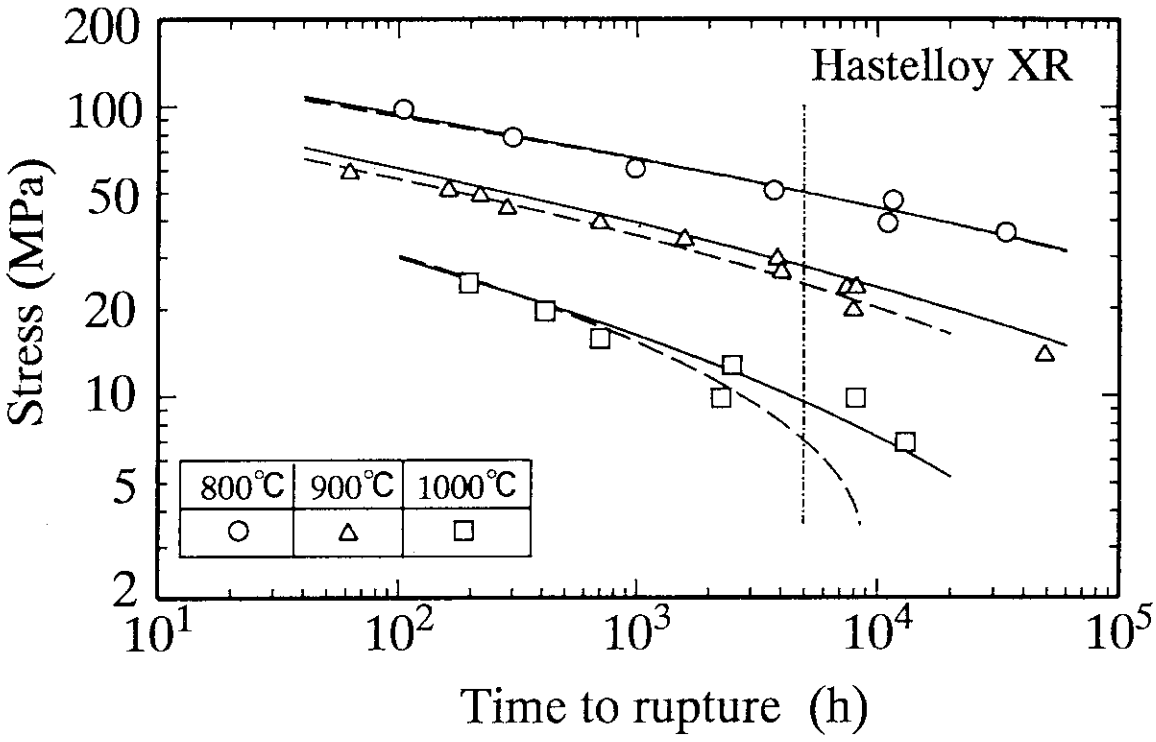

Fig. 15 Relationship between stress and time to rupture for Hastelloy XR in JAERI Type B helium. The solid lines are regression curves obtained from application of Larson-Miller Parameter(LMP)to all data points. The broken lines are those obtained from application of LMP to data points below 5,000h.

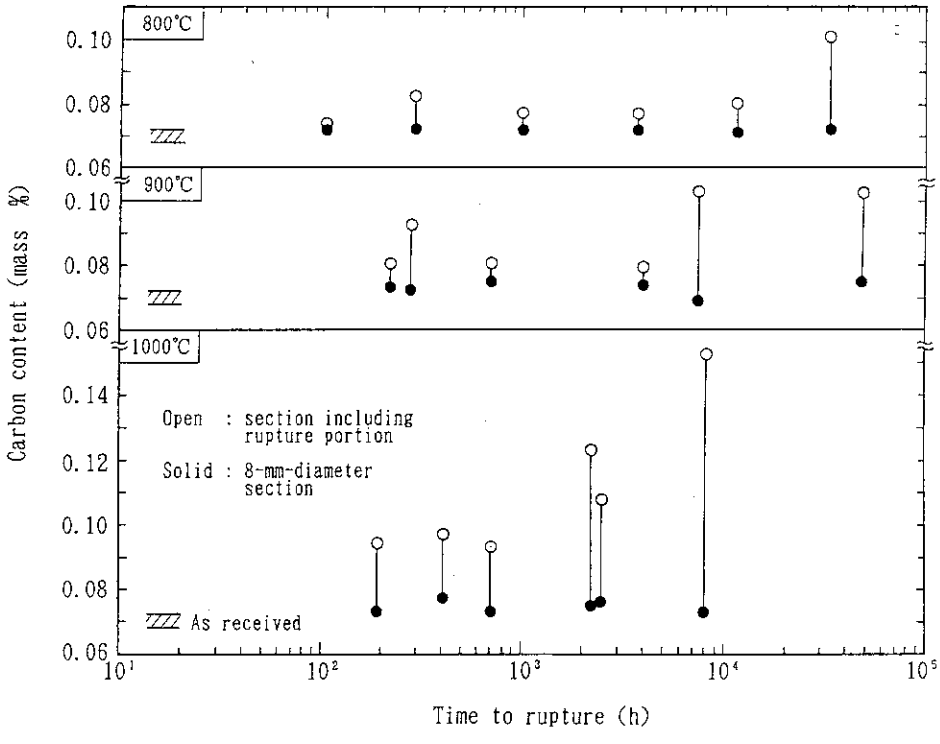

Fig. 16 Results of carbon analysis on the specimens of Hastelloy XR creep ruptured in JAERI Type B helium.

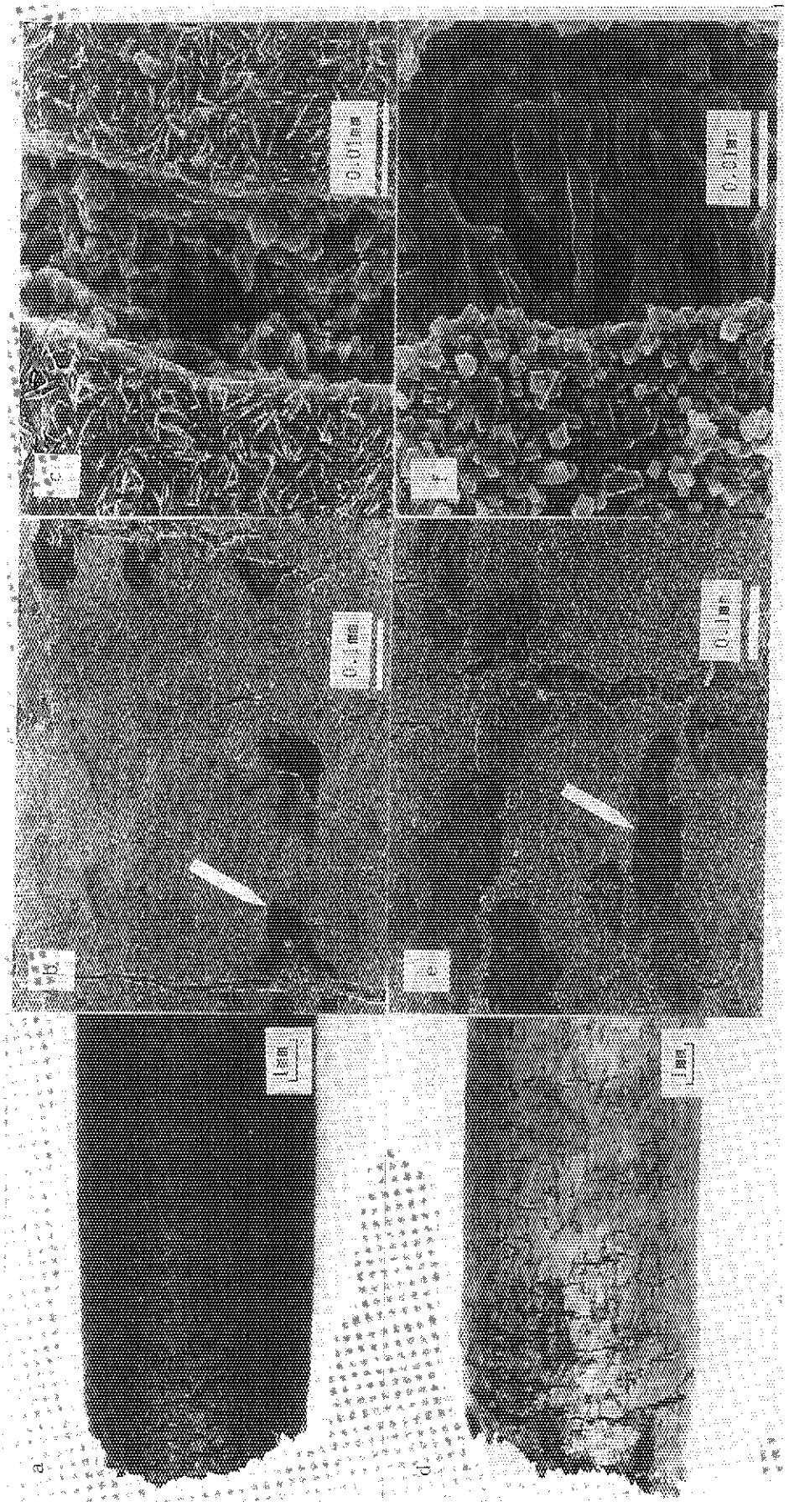

a, b and c: 800℃, 19.6 MPa, Time to rupture; 7,936.6 h
d, e and f: 1000℃, 6.9 MPa, Time to rupture; 13,014.0 h

Photo. 1 Surface topography of Hastelloy XR ruptured at 800 and 1000 ℃ in JAERI Type B helium.

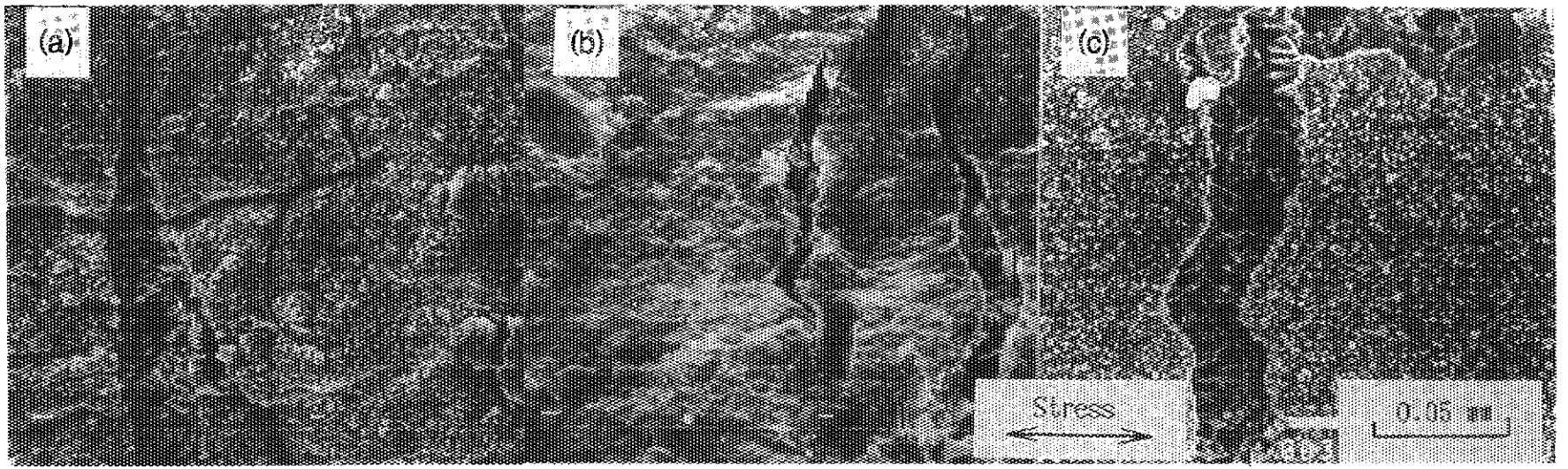

(a) 800℃, Stress : 36.3 MPa, Time to rupture : 33,521.0h

(b) 900℃, Stress : 13.7 MPa, Time to rupture : 48,587.5h

(c) 1000℃, Stress : 6.9 MPa, Time to rupture : 13,014.0h

Photo. 2 Surface topography of Hastelloy XR ruptured at 800,900 and 1000℃ in JAERI Type B helium.

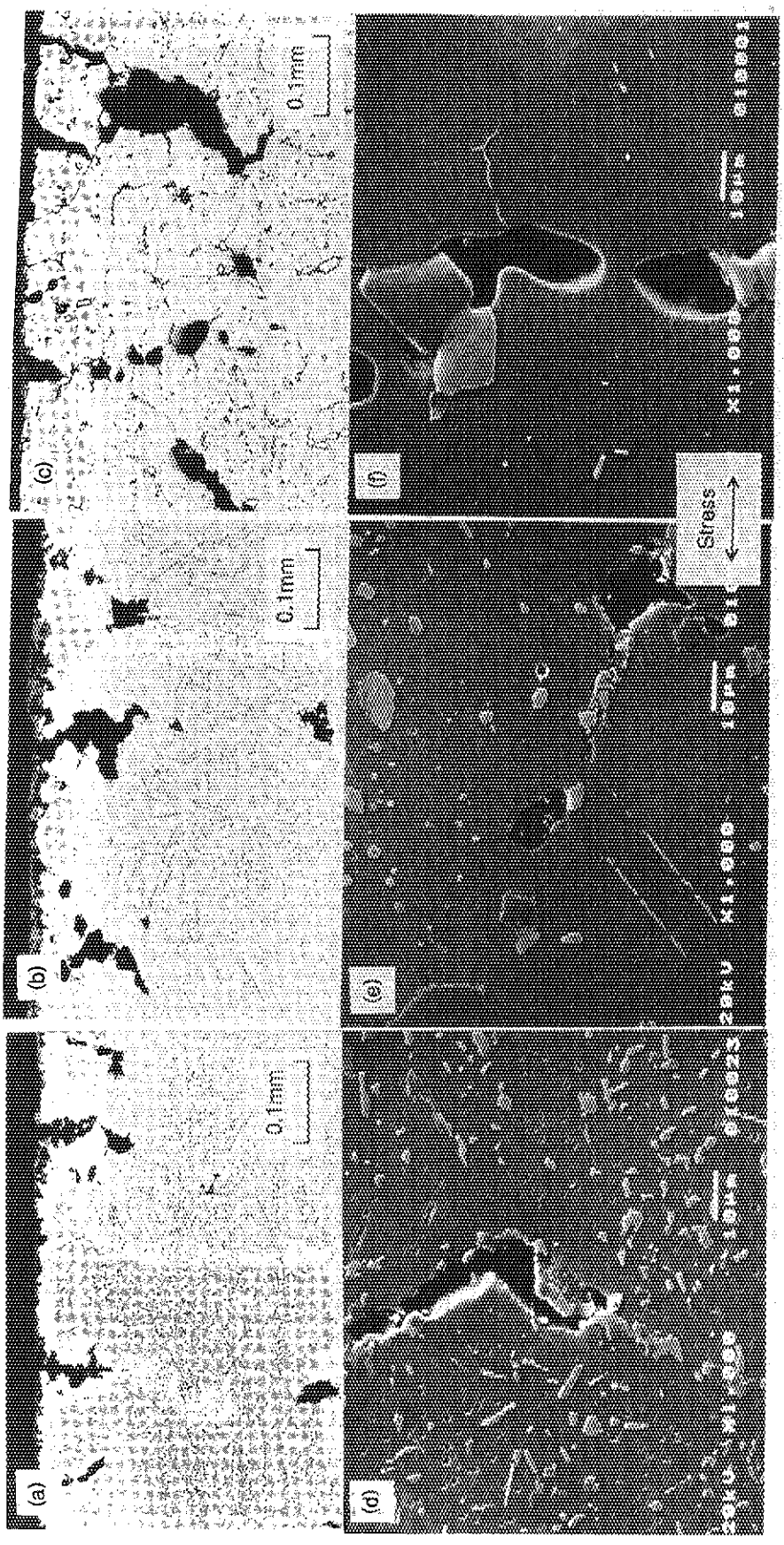

(a),(d) 800℃, Stress : 36.3 MPa, Time to rupture : 33,521.0h

(b),(e) 900℃, Stress : 13.7 MPa, Time to rupture : 48,587.5h

(c),(f) 1000℃, Stress : 6.9 MPa, Time to rupture : 13,014.0h

Photo. 3 Microstructures of Hastelloy XR ruptured at 800,900 and 1000℃ in JAERI Type B helium.

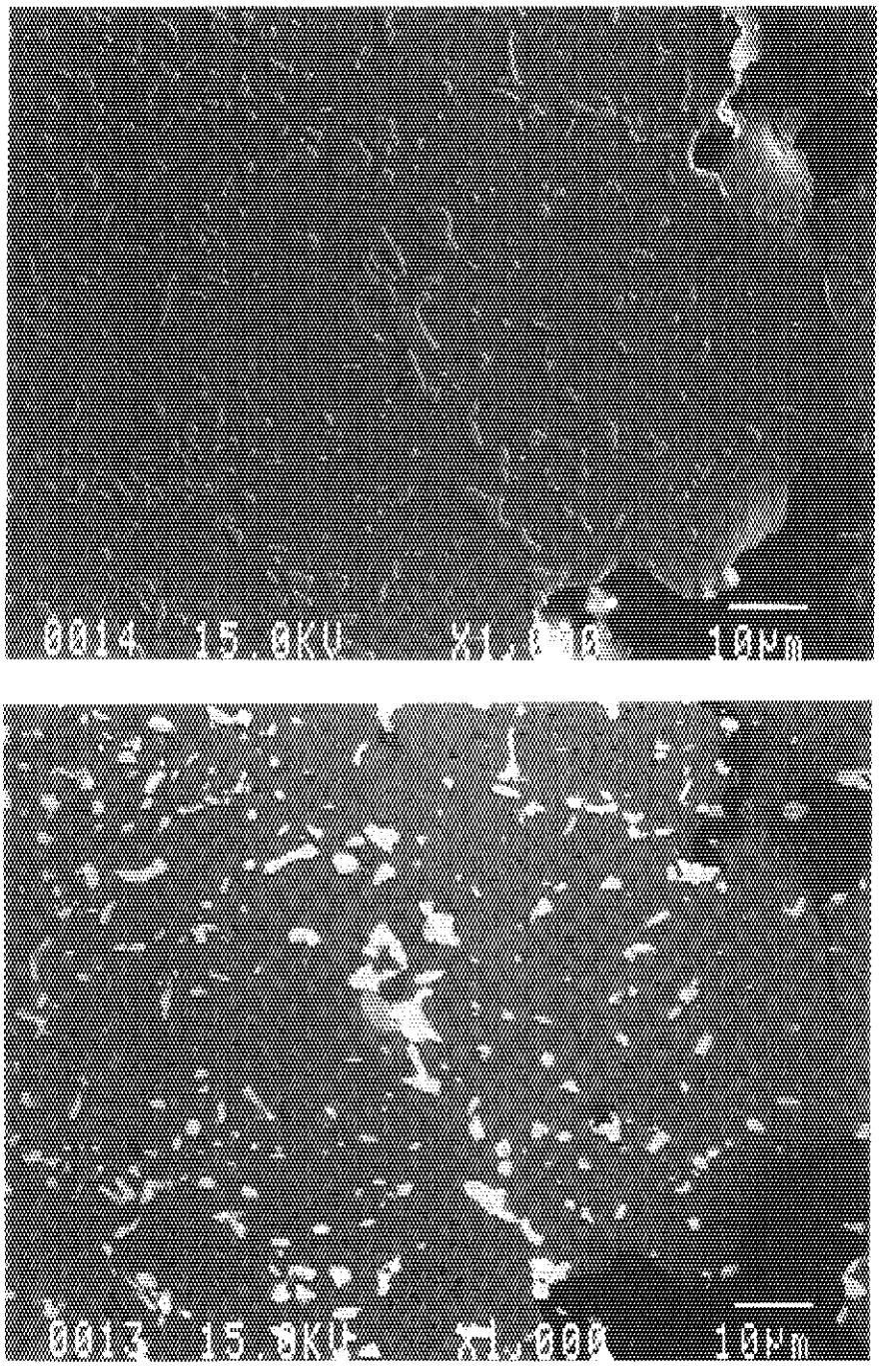

Photo. 4 Scanning electron micrographs of Hastelloy XR ruptured at 800 ℃ under 36.3 MPa.(Upper:secondary electron image, Lower: backscattered electron image)

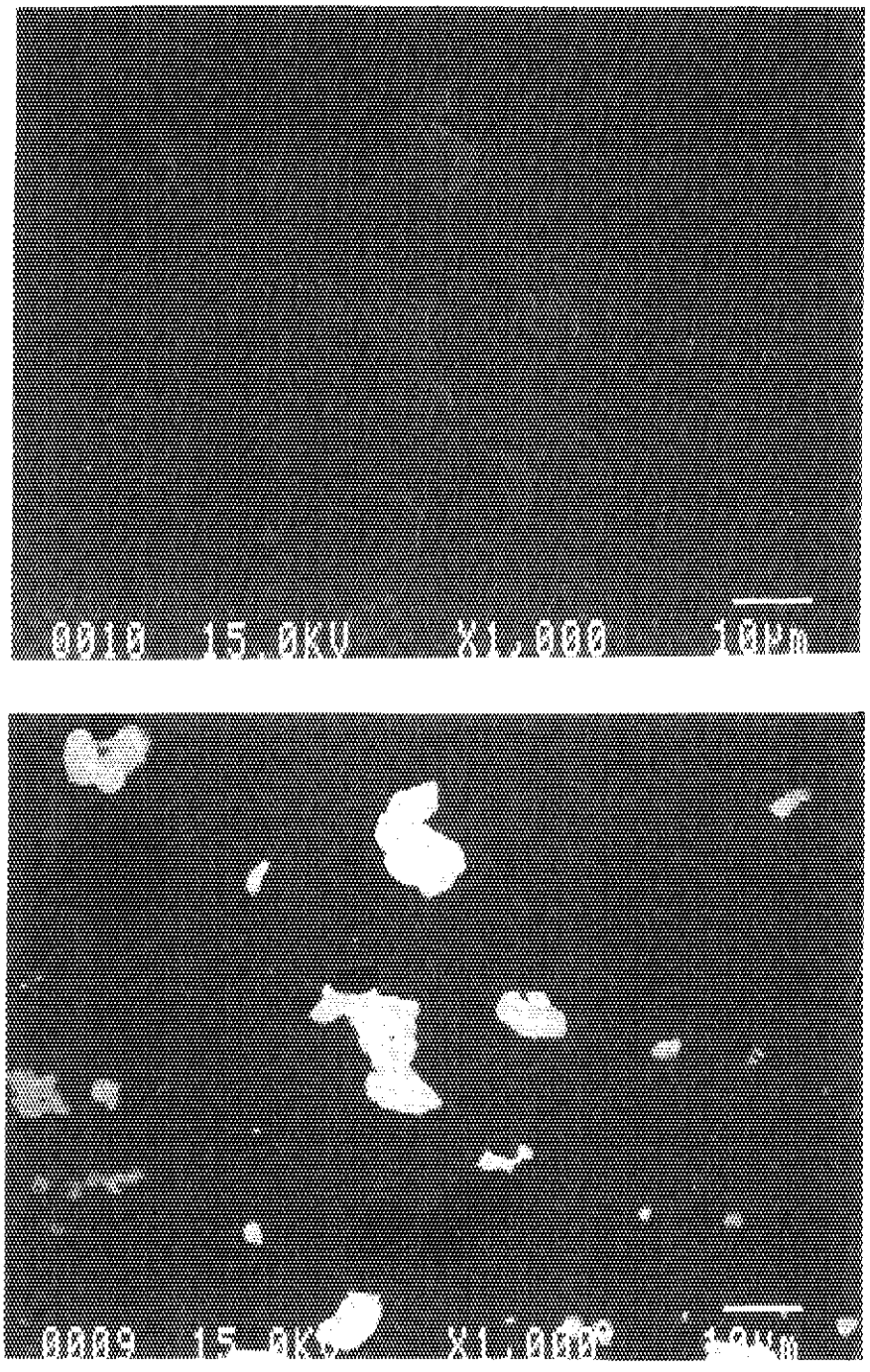

Photo. 5 Scanning electron micrographs of Hastelloy XR ruptured at 900 ℃ under 13.7 MPa.(Upper:secondary electron image, Lower: backscattered electron image)

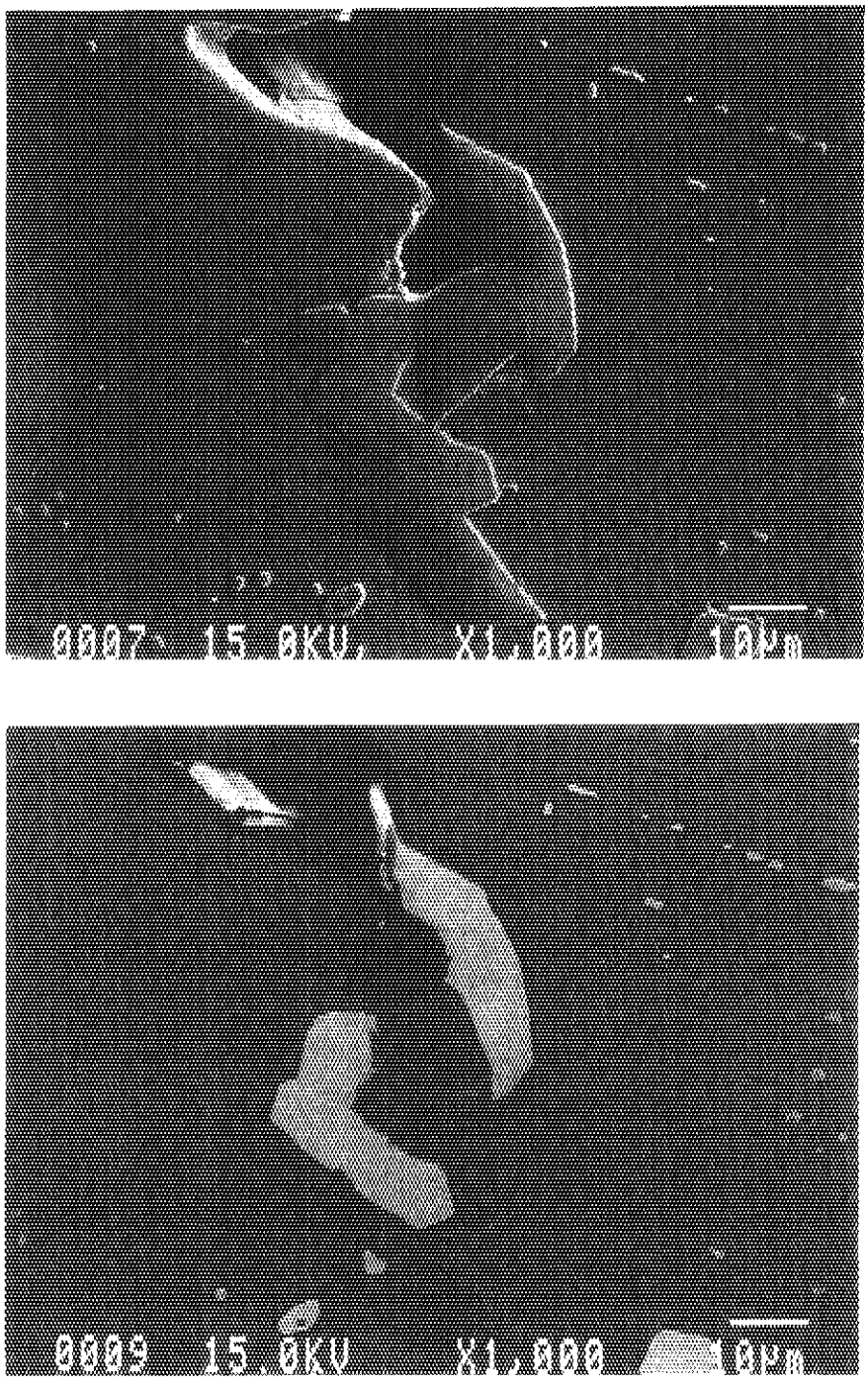

Photo. 6 Scanning electron micrographs of Hastelloy XR ruptured at 1000 ℃ under 6.9 MPa.(Upper:secondary electron image, Lower: backscattered electron image)